MICHIGAN DEPARTMENT OF COMMUNITY HEALTH
COMPUTED TOMOGRAPHY STANDARD
ADVISORY COMMITTEE (CTSAC) MEETING

Thursday, July 22, 2010

Capitol View Building
201 Townsend Street
MDCH Conference Center
Lansing, Michigan 48913

DRAFT MINUTES

I. Call to Order

Chairperson Brooks called the meeting to order at 9:35 a.m.

A. Members Present:

Rod J. Zapolski, Mid Michigan Health
Renee K. Myers, Chrysler Group LLC
James R. Pedersen, International Union UAW
Michael Altman, MD, Marquette General Health System
Suresh Mukherji, MD, Vice-Chairperson, University of Michigan Health System
Sharon L. Brooks, DDS, MS, Chairperson, Michigan Dental Association
Lawrence Ashker, DO, Genesys Regional Medical Center
Stephen Meier, Xoran Technologies Inc.
David J. Kastan, MD, FSIR, Henry Ford Health System
Daniel Shumaker, MD, FA, Michigan Radiological Society
Abdalmajid Katranji, MD, Michigan State Medical Society

B. Members Absent:

Anthony L. Alcantara, MD, St. John Providence Health System
Bradford W. Betz, MD, Spectrum Health
Robert M. Goodman, DO, Blue Cross Blue Shield/Blue Care Network

C. Michigan Department of Community Health Staff Present:

Jessica Austin
Irma Lopez
Tania Rodriguez
Stan Nash
Matt Weaver
Bruce Matkovich
Larry Horvath

II. Introductions

Member of the Committee and MDCH were introduced.

III. Declaration of Conflicts of Interests

Vice-Chairperson Mukherji stated he had been consulting with Phillips Medical Systems for the past couple of years and was a one time consultant for GE regarding their Gem Stone Technology, attending one advisory board meeting.

Mr. Meier stated that he is the general manager at Xoran Technologies which manufactures CT's.

IV. Review of the Agenda

Motion by Dr. Katranji, seconded by Vice-Chairperson Mukherji, to accept the agenda as presented.

Motion Carried.

V. Basic CON Overview

Ms. Lopez gave a basic overview of Certificate of Need (CON). (Attachment A)

Mr. Matkovich gave a brief overview of the Radiation Safety Section.

VI. Review and Discussion of Charge

Chairperson Brooks gave an overview of the Charge.

Members discussed the following:

A. Dental CT Scanners
B. Portable point of care? and mini CT scanners
C. Methodology
D. Technical changes in the language of the standards

Dr. Katranji suggested that the SAC dedicate a meeting for each charge.

VII. Background Material

Chairperson Brooks gave a written and oral summary of the following articles provided by Vice-Chairperson Mukherji and herself:

A. CBCT Machines (Attachment B)
B. Conebeam CT of the Head and Neck, Part 1: Physical Principles (Attachment C)
C. Conebeam CT of the Head and Neck, Part 2: Clinical Applications (Attachment D)

Discussion followed.

Chairperson Brooks will provide articles at the next meeting from the California Dental Association Journal, January 2010 issue and the Alpha Omegan Journal.

Chairperson Brooks would like for the DCH staff to provide the annual report data for CT scanners, and summary from the CT Public Hearing. She will look into having someone do a presentation on Radiation.

Break at 11:31 a.m. – 11:44 a.m.

VIII. Public Comments

Barbara Jackson, Blue Cross Blue Shield of Michigan
Jim Cavanaugh, Michigan Radiological Society
Dennis McCafferty, Economic Alliance for Michigan
Robert Meeker, Spectrum Health
Keith Haines, Neurologica

IX. Next Steps and SAC Workplan

Chairperson Brooks will provide a presentation on the uses in dentistry. The SAC will continue discussion on the definition, and utilization on the scanners.

Discussion followed.

X. Future Meeting Dates

August 25, 2010
September 29, 2010
October 27, 2010
November 17, 2010
December 9, 2010
January 13, 2011

XI. Adjournment

Motion by Mr. Pedersen, seconded by Vice-Chairperson Mukherji, to adjourn the meeting at 12:07 p.m. Motion Carried.

Basics of Certificate of Need (CON)
CT SAC
July 22, 2010

Certificate of Need Federal Background

- The District of Columbia and New York developed CON programs in 1964 in an effort to contain rising health care costs.
- Federally mandated CON programs were established in 1974 as a national health care cost containment strategy.

Certificate of Need Federal Background

Attachment A

- The federal mandate for CON was not renewed by the U.S. Congress in 1986.

- CON regulations are structured, in principle, to improve access to quality health care services while containing costs. Health care organizations are required to demonstrate need before investing in a regulated facility, service or equipment.

MDCH

Michigan CON Background

- Public Act 368 of 1978 mandated the Michigan Certificate of Need (CON) Program.

- The CON Reform Act of 1988 was passed to develop a clear, systematic standards development system and reduce the number of services requiring a CON.

CON Commission

- Members appointed by Governor
  - Three year terms
  - No more than six from either political party
  - Responsible for developing and approving CON review standards w/legislative oversight

- Public Act 619 of 2002 made several modifications.
  - ➢ Expanded the Commission from 5 to 11
  - ➢ Key stakeholders are now represented on the Commission (e.g., physicians)

What is Covered by the CON Program?

The following projects must obtain a CON:

- Increase in the number or relocation of licensed beds
- Acquisition of an existing health facility
- Operation of a new health facility
- Initiation, replacement, or expansion of covered clinical services

Capital expenditure projects (i.e., construction, renovation) must obtain a CON if the projects meet the following threshold:

- $2,942,500 for clinical service areas (January 2010)

Note: Threshold is indexed annually by the Department based on the Consumer Price Index.

Categories That Require CON Approval

- Air ambulances (helicopters)
- Cardiac catheterization, including diagnostic, therapeutic, angioplasty, and electrophysiology
- Hospital beds – general acute care
- Magnetic resonance imaging (MRI)
- Megavoltage radiation therapy
- Neonatal intensive care units
- Nursing home/hospital long-term care beds
- Urinary lithotripters

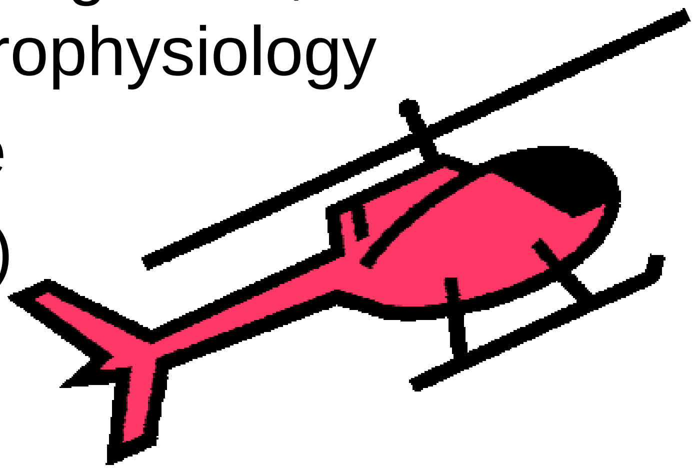

Categories That Require CON Approval

- Open heart surgery
- Positron Emission Tomography (PET)
- Psychiatric beds – acute inpatient
- Surgical services – hospital and free-standing
- Transplantation services – bone marrow, including peripheral stem cell, heart-lung, liver, and pancreas
- Computed tomography (CT) scanners

MDCH

MDCH CON Org Chart

Attachment A

Janet Olszewski, Director

Kurt Krause, Chief Deputy Director

Nick Lyon, Deputy Director, Health Policy, Health Policy and Regulation Administration

Vacant
Bureau of Legal & Policy Affairs

Stan Nash

Bill Hart, Director, Bureau of Health Policy & Access Division

Vacant (Secretary)

Health Policy Section and Commission Support

Irma Lopez, Manager

Jessica Austin

Brenda Rogers

Tania Rodriguez

Karen McCosky

Access to Care Section

Lonnie Barnett, Manager

Andy Chen

Bob Esdale

Andrew Hammontree

Ian Horste

Holly Mayes

Ken Miller

Traci Wightman

CON Evaluation Section

Larry Horvath, Manager

Rose Moye

Sallie Flanders

Andrea Moore

Tulika Bhattacharya

Perry Smith

Joette Laseur

Matt Weaver

Gaye Tuttle

Zena Flanders

Chad Thelen

Phillip Benedict

The CON Process

1. Applicant files letter of intent
2. Applicant files completed application
3. Department reviews application
4. Applicant has 15 days to submit information to DCH
5. DCH determines the review type
6. Proposed decision issued within deadlines for each review type
    - Nonsubstantive – 45 days
    - Substantive – 120 days
    - Comparative – 150 days

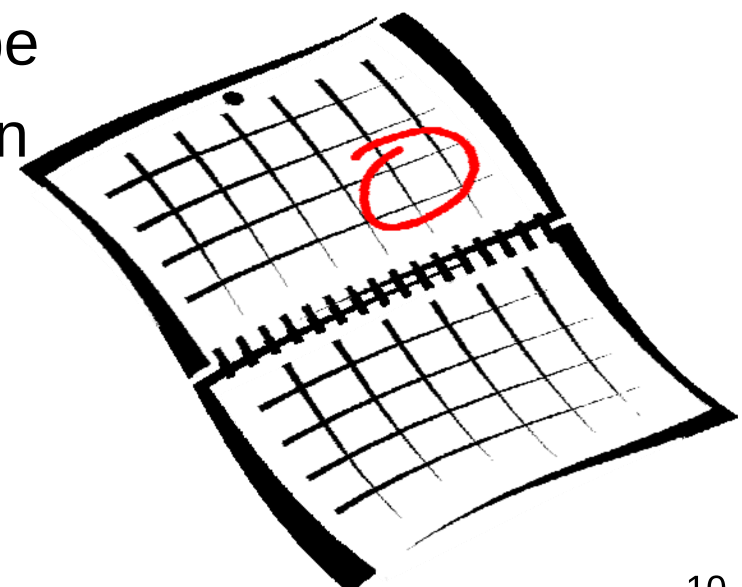

CON Process Continued…

7. Proposed decision approved

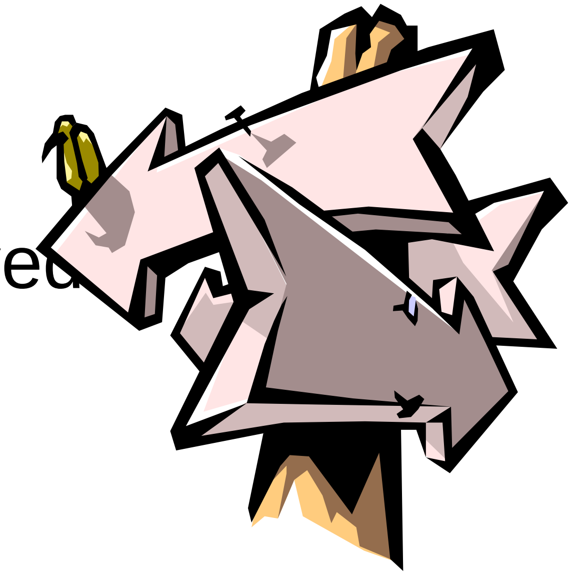

8. Proposed decision not approved

9. Hearing is not requested

10. Hearing is requested

11. DCH Director makes final decision

Statutory Authority for Review of Standards

- MCL 22215(1)(m) requires that standards be reviewed, and revised if necessary, every 3 years. Statute also requires that the Commission “If determined necessary by the Commission, revise, add to, or delete 1 or more of the covered clinical services listed in section 22203….” [MCL 22215(1)(a)]

Statutory Authority for Review of Standards Continued

- MCL 22215(1)(n) states “If a standard advisory committee is not appointed by the commission and the commission determines it necessary, submit a request to the department to engage the services of private consultants or request the department to contract with any private organization for professional and technical assistance and advice or other services to assist the commission in carrying out its duties and functions under this part.”

Standard Advisory Committee (SAC) Responsibility

- Public Health Code, Act 368 of 1978
  - MCL 333.22215 "…(1)(*l*) If the Commission determines it necessary, appoint standard advisory committees to assist in the development of proposed certificate of need review standards. A standard advisory committee shall complete its duties under this subdivision and submit its recommendations to the Commission within 6 months unless a shorter period of time is specified by the Commission when the standard advisory committee is appointed…."

MDCH

Development of the Charge

- Public Hearing in October
- Acceptance of written comments/testimony by MDCH on behalf of the Commission
- Commission members and MDCH staff review all of the comments/testimony received
- Recommendations offered to the Commission by the MDCH
- CON Commission develops and approves the final charge to the SAC

CHARGE
CT SCANNER SERVICES STANDARD ADVISORY COMMITTEE (SAC)
Approved March 9, 2010

At a minimum, the CT Scanner Services SAC is charged to review and recommend any necessary changes to the CT Scanner Services Standards regarding the following:

1) Whether or not dental CT scanners should continue to be regulated under CON. If regulation of dental CT scanners should be maintained, make recommendations, if necessary, regarding any modification to the requirements.

2) Whether or not portable point of care and mini CT scanners should continue to be regulated under CON. If regulation of portable point of care and mini CT scanners should be maintained, then make recommendation as to the requirements.

3) The methodology, e.g., volume requirements and CT equivalents in regards to CT proliferation and make any necessary recommendations.

4) Any technical or other changes from the Department, e.g., updates consistent with other CON Review standards, radiation safety issues, consistency of initiation language with Public Health Code.

SAC Operations

- Operates using modified Roberts' Rules
- Subject to Open Meeting Act; including public comment period which is placed on the agenda
- The Chair or a designee (SAC member) appointed by the Chair can run the meeting
- A physical quorum is necessary to conduct business
- Although SAC members may participate by phone; phone participation is not included in the quorum count or a vote
- A quorum is defined as a majority of the members appointed and serving
- If a quorum of the SAC members is present at any gathering, this becomes a public meeting
- Final recommendations are made by the SAC to the CON Commission. The SAC presents a written report and/or final draft language.

CON Commission Action

- Commission receives final report of the SAC
- Determines what proposed action will be taken based upon SAC recommendations

Attachment A

Legislative Oversight of Proposed Changes to CON Standards

- Any potential changes to existing standards are required to be reviewed by the Joint Legislative Committee (JLC)
- The JLC includes the chairs of the health policy committees from both the Senate and the House of Representatives
- After the CON Commission has take proposed action and no less than 30 days prior to the Commission taking final action, a Public Hearing is conducted by the Commission
- Notice of the proposed action, along with a brief summary of the impact of any changes, is provided and sent to the JLC for its review

…..Legislative Oversight Continued

- Upon the Commission taking final action, the JLC and the Governor are provided notice of the proposed final action as well as a brief summary of the impact of any changes that have been proposed by the CON Commission
- The JLC and Governor have a 45-day review period to disapprove the proposed final action. Such 45-day review period shall commence on a legislative session day and must include 9 legislative session days
- If the proposed final action is not disapproved, then it becomes effective upon the expiration of the 45-day review period or on a later date specified in the proposed final action

Attachment B

http://www.3dorthodontist.com/CBCT_Machines.html

CBCT Machines

In my opinion, the most important feature to consider when buying a CBCT scanner for orthodontic use is the scanner's largest **field of view (FOV)**. The scanner's FOV determines how much of the patient's anatomy you will be able to visualize. (See the illustration below).

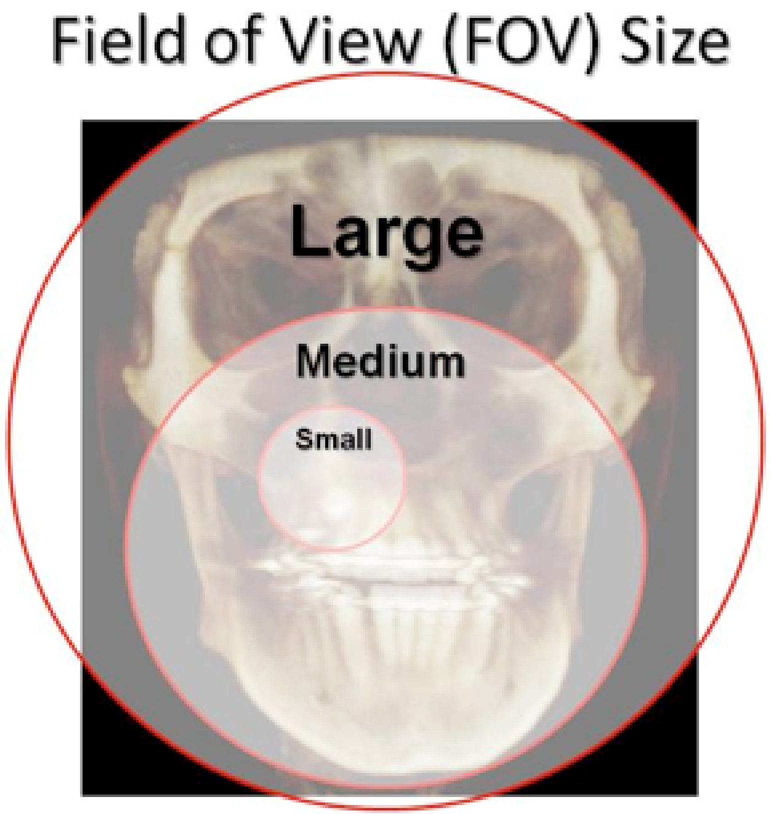

Scanners using flat panel detectors (FPD) describe the dimensions of their cylindrical FOVs as height by width (HxW). (Width can also be referred to as diameter). Scanners using image intensifiers and CCDs as their detectors (II/CCD) describe the dimensions of their spherical FOVs as cm^3. I have grouped the scanners below into three categories based on their largest FOV.

□□A scanner with a **large FOV** will show you the roof of the orbits and Nasion down to the hyoid bone. Scanners with a large FOV, usually a FOV height equal to or greater than 16 cm, are useful for cephalometrics and traditional orthodontic surveys. (Based on a typical adult male).☐☐**Medium FOV** scanners will capture the middle of the orbits down to Menton vertically, and condyle-to-condyle horizontally. Scanners with a medium FOV are useful for panos and implant surveys, but not for cephalometric analysis. ☐☐Scanners with a **small FOV** capture a user-defined region, usually symmetrical in shape. Small FOV scanners are used for implant surveys, TMJ surveys, and the localization of impacted teeth.

☐Some **combo** scanners also come with attachments for conventional 2D lateral head films and/or panoramic radiographs.☐It is also worth noting that some third-party software can **"stitch"** two small or medium FOV scans together to digitally obtain a larger FOV, (e.g., Anatomage's InVivoDental & Dolphin Imaging's Dolphin 3D).☐☐Click on the model's name below to be directed to these third-party websites:

LARGE FOV CBCT SCANNERS

Model	Manufacturer	Max. FOV (HxW) (cm)	Min. Voxel (mm)	2D Options	Notes
Next Generation (Platinum) i-CAT	Imaging Sciences International	17x23	0.125	Pano	
Classic i-CAT	Imaging Sciences International	16x22	0.2	No	
NewTom 3G	AFP Imaging	20x20x20	0.2	No	
CB MercuRay	Hitachi Medical	20x20x20	0.2	No	
Quolis Alphard 3030	Asahi Roentgen	18x20	0.125	No	

	(Belmont)				
3D eXam	KaVo	17x23	0.125	?	
Kodak 9500	Kodak Dental Systems	18x21	0.2	No	Also available in a MFOV
ProMax 3D Max	Planmeca	17x22	0.125	No	Can obtain a stitched 22x22 cm FOV
Picasso Master 3D	E-WOO	19x20	0.2	No	
Picasso Master 3DS	E-WOO	19X20	0.165	No	

MEDIUM FOV CBCT SCANNERS

Model	Manufacturer	Max. FOV (HxW) (cm)	Min. Voxel (mm)	2D Options	Notes
NewTom 9000	Aperio Services	15x15x15	0.3	No	Discontinued - No link available
NewTom VG*i*	AFP Imaging	15x15	0.15	No	
NewTom VG*i* Flex	AFP Imaging	15x15	0.15	No	Intended for mobile use
Galileos Compact	Sirona	12x15x15	0.3	No	
Galileos Comfort	Sirona	15x15x15	0.15	No	
Scanora 3D	Soredex	7.5x14.5	0.133	Pano	Can obtain a stitched 13x14.5 cm FOV
SkyView	MyRay	15x15x15	0.16	No	
GXCB-500	Gendex	8x14 (using EDS)	0.125	No	Powered by i-CAT
GXCB-500	Gendex	8x14	0.125	Yes	Powered by i-CAT

HD		(using EDS)			
MiniCAT	Xoran Technologies	12x17	0.2	No	
Picasso Trio	E-WOO	7x12	0.125	Pano/Ceph	
Picasso Pro	E-WOO	7x12	0.125	No	No longer available in the USA
Iluma	IMTEC (3M)	14X21	0.09	No	
xCAT ENT	Xoran Technologies	14x24	0.4	No	Specialized for intraoperative use
PaX-Reve3D	E-WOO	15x15	0.25	Pano/Ceph	Optional 15x19 FOV
3D Accuitomo 170	J. Morita	12x17	0.08	No	

SMALL FOV CBCT SCANNERS

Model	Manufacturer	Max. FOV (HxW) (cm)	Min. Voxel (mm)	2D Options	Notes
ProMax 3D	Planmeca	8x8	0.16	Pano/Ceph	Can obtain a stitched 14x14 cm FOV
PreXion 3D	PreXion, Inc.	8x7.5	0.1	No	Previously owned by TeraRecon. (Marketed as FineCube by Yoshida Dental in Japan)
AUGE ZIO	Asahi Roentgen	7x8	0.125	Pano/Ceph	This model comes in 6 versions with varying features

9000 3D	Kodak Dental Systems	4x5	0.076	Pano	
9000 3DC	Kodak Dental Systems	4x5	0.076	Pano/Ceph	
Picasso Duo	E-WOO	8x8	0.2	Pano	Marketed as PaX-Duo3D in Korea with 12x8.5 FOV
PaX-500 ECT	VATECH	5x5	0.186	Pano/Ceph	Various versions available
PaX-Uni3D	VATECH	5x8	0.186	Pano/Ceph	Various versions available
CB Throne	Hitachi Medical	10x10x10	0.125	No	Not available in the USA
3D Accuitomo	J. Morita	3x4	0.125	No	Uses a II/CCD sensor
3D Accuitomo FPD	J. Morita	6x6	0.125	No	Uses FPD sensor
3D Accuitomo 80	J. Morita	8x8	0.08	No	
Veraviewepocs 3D 40	J. Morita	4x8	0.125	Pano/Ceph	Various configurations available
Veraviewepocs 3D 80	J. Morita	8x8	0.125	Pano/Ceph	Various configurations available
Veraviewepocs 3De	J. Morita	4x8	0.125	Pano/Ceph	Various configurations available

Suni3D	Suni Medical Imaging	5x8	0.2	Pano/Ceph	
ORION RCB-888	Ritter Imaging	8.5x8.5	0.1	No	
Finecube XP62	Yoshida	7.5x8.1	0.1	No	Marketed as PreXion 3D by PreXion Inc. in the USA

Please feel free to use the lists above from my website. I only ask that you credit my website when doing so since it takes countless hours to compile and maintain these lists.

Am I missing a cone-beam CT scanner or do you have a correction? Click here to let me know.

REVIEW ARTICLE

Conebeam CT of the Head and Neck, Part 1: Physical Principles

A.C. Miracle
S.K. Mukherji

SUMMARY: Conebeam x-ray CT (CBCT) is a developing imaging technique designed to provide relatively low-dose high-spatial-resolution visualization of high-contrast structures in the head and neck and other anatomic areas. This first installment in a 2-part review will address the physical principles underlying CBCT imaging as it is used in dedicated head and neck scanners. Concepts related to CBCT acquisition geometry, flat panel detection, and image quality will be explored in detail. Particular emphasis will be placed on technical limitations to low-contrast detectability and radiation dose. Proposed methods of x-ray scatter reduction will also be discussed.

Conebeam x-ray CT (CBCT) is a relatively recent installment in the growing inventory of clinical CT technologies. Although the first prototype clinical CBCT scanner was adapted for angiographic applications in 1982, the emergence of commercial CBCT scanners was delayed for more than a decade.[1] The arrival of marketable scanners in the last 10 years has been, in part, facilitated by parallel advancements in flat panel detector (FPD) technology, improved computing power, and the relatively low power requirements of the x-ray tubes used in CBCT. These advancements have allowed CBCT scanners to be sufficiently inexpensive and compact for operation in office-based head and neck as well as dental imaging applications. These systems are distinguished by a conical x-ray beam geometry and the use of 3D reconstruction algorithms; most recent models are also fit with FPDs. As they are employed for specific imaging tasks in restricted anatomic regions such as the head and neck, preliminary research suggests that they can produce images with high isotropic spatial resolution while delivering a relatively low patient dose. This first part in a series of 2 articles will review the physical principles underlying CBCT as it is employed in head and neck diagnostic imaging. C-arm CBCT systems used in the interventional suite and CBCT systems used in radiation therapy have been the subject of other reviews.[2-4] Although there are numerous differences between CBCT and conventional fan-beam CT techniques, many of the fundamental physical concepts are the same.

Fundamental Principles of CT

The original clinical CT scanner was introduced by Sir Godfrey N. Hounsfield in 1967. Data acquisition was based on a translate-rotate parallel-beam geometry wherein pencil beams of x-rays were directed at a detector opposite the source and the transmitted intensity of photons incident on the detector was measured. The gantry would then both translate and rotate to capture x-ray attenuation data systematically from multiple points and angles.[5] Although x-ray sources, acquisition geometries, and detectors have rapidly evolved since Hounsfield's original scanner, the theory behind CT has not changed.

From the Departments of Radiology (A.C.M., S.K.M.), Otolaryngology (S.K.M.), and Radiation Oncology (S.K.M.), University of Michigan Health System, University Hospital, Ann Arbor, Mich.

Please address correspondence to Aaron Miracle, University of Michigan Medical Center, Department of Radiology, B2B311 UH SPC 5030, 1500 East Medical Center Dr, Ann Arbor, MI 48109-5030; e-mail: amiracle@med.umich.edu

Indicates open access to non-subscribers at www.ajnr.org

DOI 10.3174/ajnr.A1653

The attenuation of a monochromatic x-ray beam through a homogeneous object is described by the Lambert-Beer law:

$$I = I_o e^{-\mu x},$$

where I is the transmitted photon intensity, I_o is the original intensity, x is the length of the x-ray path through the object, and μ is the linear attenuation coefficient of the material traversed. This expression changes for inhomogeneous materials such as human tissue:

$$I = I_o e^{-\int \mu x dx}.$$

Line integrals of the linear attenuation coefficients, μ, can be obtained by taking the negative logarithm of the above expression. A line integral at angle θ through the object is the ray sum, a set of which at a given θ constitutes a projection. The computational problem in CT is to determine μ at a given point from a large set of projections obtained at varying θ about the object, a computation based on the theory formulated by Radon in 1917.[6]

Data acquisition in conventional CT imaging has evolved through 4 generations of acquisition geometries. First-generation scanners used parallel pencil beams of x-rays and required both translation and rotation of the source and a single-detector apparatus. Second-generation scanners introduced fan-beam x-ray geometry and used a single-detector linear array. In third-generation scanners, the single-detector arc was introduced in conjunction with fan-beam x-ray geometry. Fourth-generation scanners used a fan-beam of x-rays and a circular detector array. In current practice, multidetector helical CT (MDCT) scanning is most frequently used, answering the call for reduced acquisition times. MDCT is loosely based on third-generation geometry, though the detector array has multiple rows of detectors.

CBCT

The discussion below will highlight the physical principles underlying CBCT as they contrast with conventional MDCT. A commercially available CBCT system designed for point-of-service head and neck diagnostic imaging will be used as an example (MiniCAT; Xoran Technologies, Ann Arbor, Mich). This system is depicted in Fig 1. Similar systems for office-based dentomaxillofacial applications have been available since 2001.[7]

Data Acquisition

In CBCT systems, the x-ray beam forms a conical geometry between the source (apex) and the detector (base) (Fig 2). This

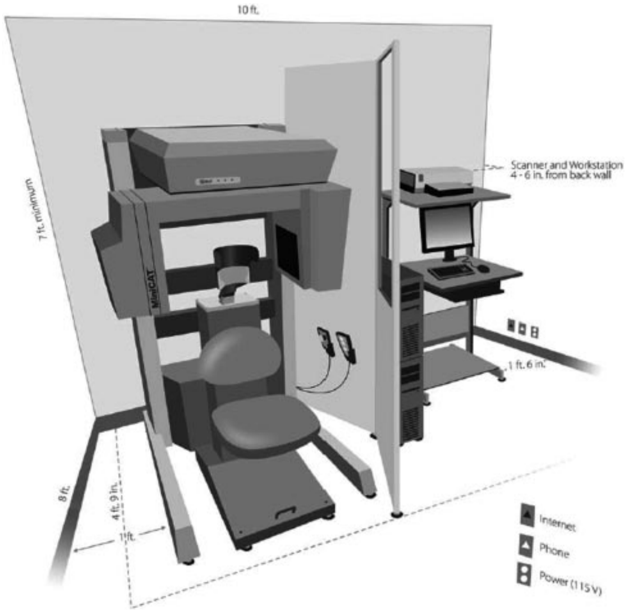

Fig 1. Schematic of an office-based CBCT scanner dedicated for extracranial head and neck imaging applications (MiniCAT). Reprinted with permission of Xoran Technologies, Ann Arbor, Mich.

is in contrast to conventional fan-beam geometry (Fig 2), in which the collimator restricts the x-ray beam to approximately 2D geometry. In a fan-beam single-detector arc geometry, data acquisition requires both rotation and z-direction translation of the gantry to eventually construct an image set composed of multiple axial sections. In CBCT systems using a 2D FPD, however, an entire volumetric dataset can be acquired with a single rotation of the gantry. Incident photons on multiple-row detectors in MDCT actually fall on a 2D area of detectors, as with flat-panel detection; indeed, with increasing numbers of rows in MDCT detector arrays, the acquisition geometry actually approximates that of a conebeam system.

FPDs

Digital FPDs enable the direct conversion of x-ray energy into a digital signal with high spatial resolution. The fundamental design consists of a screen of scintillator crystals grown onto a matrix of photodiodes embedded in a solid-state amorphous silicon (aSi:H) or selenium layer. Incident x-rays are photochemically converted to light by the scintillator film and transmitted directly to the photodiode array where the signal-intensity charge is stored. Thin-film transistors fabricated into the aSi:H matrix relay a signal intensity proportional to the stored charge in the photodiode array, which is, in turn, proportional to the incident photons on the scintillator layer. The FPD used in the MiniCAT is an indirect-conversion system based on a cesium iodide (CsI) scintillator embedded in an aSi:H layer. CsI scintillators produce superior spatial resolution owing to the microscopic columnar structure of the CsI substrate, which serves essentially as a fiber-optic conductor for the signal intensity being transmitted to the photodiode array.[8] FPD arrays afford greater spatial resolving potential with similar noise intensity when compared with their x-ray intensifier/charge-coupled device (CCD) predecessors.[9]

Reconstruction Algorithms

Reconstruction algorithms in tomographic imaging are concerned with producing multidimensional images through the inversion of 1D projection data. The reconstruction algorithm most frequently used in CBCT is a modified Feldkamp algorithm.[8] The Feldkamp algorithm is essentially a 3D adaptation of the filtered backprojection method used in fan-beam 2D reconstructions.[10,11] The process of filtering, or convolution, involves applying a kernel, or mathematic filter, to raw projection data before it is backprojected. Filtering reduces the blur otherwise inherent in the process of backprojection. The early Feldkamp algorithms solved the inversion problem for acquisition involving full circular rotation of the conebeam vertex about the object. More recent algorithms have been adapted for short circular arc trajectories of the x-ray source.[12]

A primary teleologic difference between CBCT and MDCT is the isotropic nature of acquisition and reconstruction in conebeam systems. In a CBCT system with 2048 × 1536 detector elements—similar to the 1920 × 1536 elements in the MiniCAT detector—for example, reconstruction produces a volumetric dataset with isometric voxels as small as 150 ×

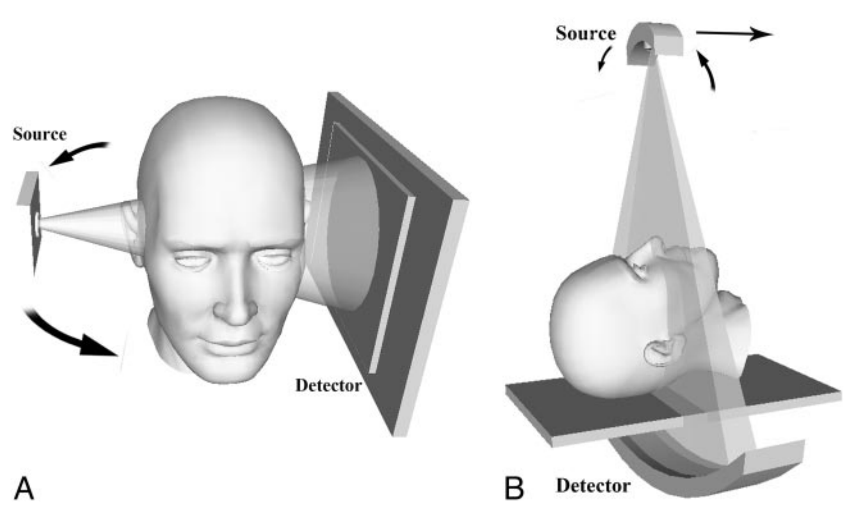

Fig 2. Depiction of CT acquisition geometries. *A*, Conebeam geometry in a compact office-based system designed for the patient to sit upright. *B*, Conventional fan-beam geometry as it is used in MDCT scanners with the patient supine.

Fig 3. Clinical images of 2 patients acquired with the MiniCAT dedicated head and neck CBCT scanner. *A*–*C*, Axial, sagittal, and coronal images, respectively, of a patient's normal temporal bones acquired with a temporal bone protocol (40 seconds, 600 frames, 0.3-mm pixels, 125 kVp, 50.85 mA). Voxels are isometric, allowing reconstruction with equally high fidelity in the 3 depicted planes. *D*–*F*, Coronal, axial, and sagittal images, respectively, of the paranasal sinuses of a patient with mild mucosal thickenings. These images are acquired with a sinus protocol (40 seconds, 600 frames, 0.4-mm pixels, 120 kVp, 48 mA).

$150 \times 150\ \mu m^3$ at the isocenter.[2,8] Images can then be constructed in any plane with high fidelity (Fig 3). MDCT reconstruction produces individual sections, which are then stacked. Compared with MDCT, in which $500 \times 500\ \mu m^2$ in-plane and 500- to 1000-μm z-axis resolutions are expected, CBCT theoretically reduces the effect of partial volume averaging[13] and can improve the spatial resolution of high-contrast structures in any chosen viewing plane.

Image Quality

Several physical descriptors and parameters are commonly enlisted to characterize the quality of an image. In characterizing CT systems, quantum noise, spatial resolution, contrast resolution, and detector quantum efficiency (DQE) are of particular interest. Quantum noise is fundamentally related to image quality and is a function of dose, tissue transmissivity, and voxel size. Noise is, in turn, a principal determinant of contrast resolution and, to a lesser extent, spatial resolution, which, along with artifacts, constitute the major observable determinants of overall image quality. CBCT imaging with FPD technology typically affords excellent spatial resolution with a relatively low patient dose. Contrast resolution suffers, however, due to increased x-ray scatter and the reduced temporal resolution and dynamic range of the FPDs.[2] The discussion below will highlight the physical characteristics relevant to CBCT imaging and the extent to which they impinge on image quality. Scatter will be addressed in detail due to its particular impact on contrast resolution. Dynamic range and temporal resolution will also be addressed in addition to several proposed approaches to improvements in CBCT image quality.

Scatter

Increased x-ray scatter represents one of the primary technical obstacles in CBCT imaging, limiting image quality in comparison with MDCT. Scatter refers to the off-axis low-energy radiation that is generated in the patient during image acquisition. It corresponds to the contribution to photon fluence at the detector not attributable to the incident primary beam. In conventional fan-beam MDCT, collimation at the x-ray source restricts the z-axis coverage of the beam, only allowing scatter from a thin axial volume of tissue to reach the detector elements during section acquisition. In contrast, CBCT expands the z-axis coverage of the beam, allowing x-ray scatter generated from the entire volume of coverage to reach the detector elements as the image is acquired. The emission characteristics of the MiniCAT x-ray source are depicted in Figure 4.

Scatter contribution is expressed as the scatter-to-primary ratio (SPR) and can be as high as 3 in large-volume CBCT systems compared with ~0.2 in conventional MDCT systems.[14] Increased scatter not only amplifies patient dose but is a principal contributor to reduced contrast resolution and increased noise in CBCT images. Streak and cupping artifacts (lower voxel values at the image center) can also be produced, further degrading image quality.[15] In an effort to improve the contrast-to-noise ratio (CNR) and reduce image artifacts,

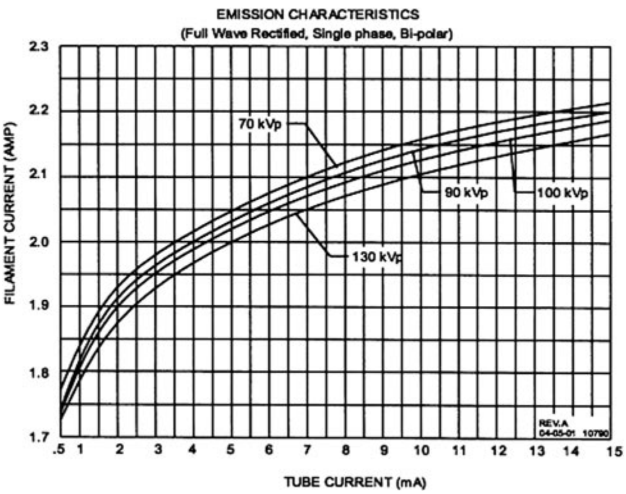

Fig 4. Emission characteristics of the MiniCAT x-ray source, manufactured by Source-Ray, Inc. (Bohemia, NY). The tube voltage range is 60–125 kVp (manufacturer's data). Reprinted with permission of Xoran Technologies, Ann Arbor, Mich.

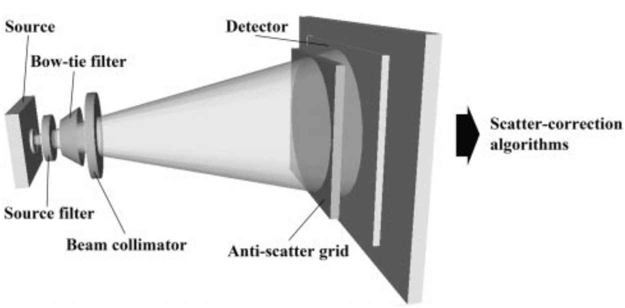

Fig 5. Schematic depiction of the methods for reducing and subtracting x-ray scatter from total photon fluence at the detector. Methods are depicted in a series and include source filtration, compensating filtration (bow tie filter), beam collimation, antiscatter grids, and scatter-subtraction preprocessing algorithms.

multiple approaches to scatter reduction have been investigated and will be discussed below (Fig 5).

The modifiable contributors to scatter generation are the imaging geometry (intervening air space or air gap), the z-direction coverage in the field of view (FOVz), and the energy profile of the x-ray beam.[16] To this end, the most basic approaches to scatter reduction are to minimize the FOVz, maximize the air gap, and optimally collimate and modulate the x-ray beam. Unfortunately, FOVz and air gap are dependent on the tissue volume of interest and the spatial limitations of the system gantry, respectively, and, thus, are limited in their ability to minimize scatter. That said, it is still important to select the smallest FOVz possible while continuing to provide adequate target-tissue coverage. Spatial restrictions limit the practicality of further increasing the air gap to reduce scatter, especially in office-based head and neck scanners designed to be compact.

Collimation and Source Filtration

X-ray filtration at the source, beam collimation, and compensating filtration constitute direct methods of scatter reduction. Filtration at the source can be achieved by applying an aluminum filter to remove low-energy photons uniformly from the x-ray beam. Beam collimation eliminates photons outside the intended FOVz, reducing the contribution of peripheral scatter to the SPR in the FOV.[8]

Compensating Filtration

The x-ray path length through tissue at the edges of the FOV is typically shortened in relation to the structure of the scanned object. This results in less attenuation of peripheral scatter and, thus, disproportionately increased peripheral scatter contribution to image degradation. Peripheral scatter not only constitutes the largest contribution to total scatter but forms the basis of the cupping artifact, the effect of which can be mitigated by compensating filtration.[15] The bow tie or wedge filter is the prototypical compensating filter used in CBCT systems. It modulates the beam profile by increasing photon density at the center of the cone and decrementally reducing density at the periphery. In the radiation therapy CBCT literature, Graham et al[15] were able to demonstrate a >50% reduction in scatter with the implementation of copper bow tie filters. Image-quality improvement has been described with bow tie filters in a CBCT system integrated into the gantry of a conventional CT scanner as well.[8] Compensating filtration is not without criticism, however, because beam hardness has been shown to negatively impact detector efficiency, as demonstrated by a decrease in the ratio of the output signal intensity–to-noise ratio (SNR) to the entrance exposure (SNR/entrance exposure).[17] The kilovolt (peak) (kVp), which is related to the beam hardness, has also been shown to produce optimal low-contrast detectability when it is kept at lower settings.[18] Thus, although scatter and cupping artifacts may be reduced with bow tie filters, this reduction may come at the expense of detector efficiency and low-contrast detectability.

Compensating filtration and the other direct scatter-reduction methods at the source side of the apparatus have the added appeal of reducing patient dose and can, of course, be used in series.[8]

Antiscatter Grids

Antiscatter grids represent an alternative method of direct scatter reduction that has been used with FPDs in digital radiographic and fluoroscopic imaging for some time.[19] Rather than modulating the beam properties at the source, a grid of lead leaves is fitted over the detector to preferentially absorb off-axis radiation not contributing to primary photon fluence. In CBCT systems, the lead leaves are arranged in a radial pattern centered on the focal spot of the FPD. Antiscatter grids have been evaluated in several experimental CBCT systems with mixed results.[8,16,19,20] A reduction in both cupping artifact and overall scatter has been observed,[8,16] though there may be insufficient improvement in contrast and observed image quality to warrant use except in situations of high scatter.[16,19] Siewerdsen et al[16] evaluated antiscatter grids in a linear accelerator-coupled CBCT system and found that image quality and CNR improved only in situations of high scatter—such as with a large FOVz covering a large anatomic site—or in input quantum-limited situations such as with high dose or low spatial resolution. To the extent that antiscatter grids improve soft-tissue contrast and artifacts, they also increase noise, which leads to a degradation in overall image quality. An escalation in dose or reduction in spatial resolution is needed to offset the increased noise with the implementation of grids. For a relatively small FOVz, such as that used in a targeted head and neck scan, antiscatter grids may improve image contrast and reduce cupping artifacts, but the increased noise requires that the dose be increased or spatial resolution be decreased to produce a high-quality image with a favorable CNR.[16]

Scatter Correction Algorithms

Some sort of scatter subtraction or homogenization preprocessing algorithm is used in most clinical CBCT systems.[2,3,21] Several approaches have been studied, including Monte Carlo simulations, blocker-based or beam-stop techniques, analytic calculations, and collimator shadow estimation.[22-24] Perhaps the most theoretically robust algorithm is that based on the Monte Carlo simulation, which predicts scatter on the basis of a voxel density model of the entire acquired tissue volume during preprocessing.[22,25] The predicted scatter contribution at each detector element is then subtracted before reconstruction. Monte Carlo simulations still require significant computation time, however, which has fueled continued research in other algorithmic approaches. Methodologically, algorithms do not reduce the additional patient dose attributable to scatter, but they have been able to achieve significant improvements in image uniformity, CNR, and CT number accuracy.[22,25] They can, of course, be implemented in conjunction with other direct methods of scatter reduction.

Dynamic Range

Dynamic range, a quality of the detector, refers to the range of incident signal intensities that can be successfully captured and transmitted as image data. A large detector dynamic range generally corresponds to improved contrast resolution. Although the dynamic range of aSi:H FPDs exceeds that of x-ray intensifier/CCD detectors, it is still slightly inferior to the ceramic detectors used in MDCT.[8] Solid state aSi:H FPDs are characterized by a dynamic range of $\sim 10^4$:1, digitized into a 14-bit readout, compared with $\sim 10^6$:1 for ceramic scintillation material in MDCT detectors.[26,27] To realize the full dynamic range potential of aSi:H FPDs, Roos et al[27] described an FPD with a dynamic gain-switching mode, effectively increasing the dynamic range by a factor of 6. Image acquisition in dynamic gain-switching mode extends the dynamic range to 16 bits and can enable contrast resolution of 3 Hounsfield units (HU), which rivals that of MDCT and exceeds the 5- to 10-HU low-contrast detectability typically quoted for current CBCT systems.[3,8,21]

Temporal Resolution

Temporal resolution refers to the ability of an imaging system to discriminate sequentially acquired projection data separated by small time intervals. With higher temporal resolution, more projection datasets can be acquired over a fixed gantry rotation interval, thus improving contrast resolution. As it applies to contrast resolution, FPDs have inherently limited temporal resolution compared with the ceramic detectors used in MDCT systems.[2] Limited temporal resolution leads to image ghosting and "after-glow" or memory effects as well as streak artifacts, which degrade image quality and impair low-contrast detectability.[28]

Limited temporal resolution at fixed gantry speeds in CBCT with FPD systems is related to the characteristics of the scintillator materials. CsI is a relatively slow scintillator susceptible to the after-glow effect, wherein the detector response to a new exposure is overwhelmed by the after-glow of the previous exposure, particularly if that exposure was transmitting high signal intensity such as with high-contrast structures.[29] This restricts the acquisition speed of the scanner in order that ghost images from after-glow can be minimized, thus placing a limit on gantry rotation speed and overall data-acquisition time. Subtracting a fraction of the previous image during preprocessing can help minimize this effect.[8]

Spatial Resolution

The spatial resolution of an imaging system is its ability to discriminate objects of different attenuation at small separation distances. It is typically described as the spatial frequency (measured in line pairs per centimeter [lp/cm]) that can be discriminated with a 10% detection of true contrast. The "modulation transfer function" (MTF) relates the percentage of actual contrast conferred to the spatial frequency of inserts in a phantom and is the product of the Fourier transform of a composite of functions describing image blur, unsharpness, and contrast response in reference to the ability to resolve line pairs per unit length. Spatial resolution is determined primarily by the inherent blurring in the detection apparatus and the individual area of the detection elements.[26] "Binning" refers to the process of grouping detector elements together for the transmission of 1 uniform signal; 1×1 binning affords the greatest ultimate spatial resolution but at the expense of the SNR if the dose is held constant. Improved SNR is possible with 2×2 and larger binning sizes. Superior spatial resolution is one of the most attractive qualities of CBCT imaging and is largely the result of FPD technology and isotropic data acquisition.

For images acquired at 125 kVp and reconstructed with a sharp kernel, the MiniCAT temporal bone protocol discriminates a spatial frequency of 14–16 lp/cm with 10% contrast detection (personal communication with Rohini Rebello-D'Souza, September 25, 2008). The MTF curves for images acquired under several MiniCAT protocols are depicted in Fig 6. Gupta et al[8] have described spatial resolutions of 22–24 lp/cm in images acquired at 120 kVp with 2×2 binning of the detector elements in an FPD CBCT system as well. This spatial resolution corresponds to isometric voxels the size of a 200- to 250-μm cube. As mentioned under "Reconstruction Algorithms" above, isometric voxels as small as $150 \times 150 \times 150$ μm^3 at the isocenter have been achieved.

DQE

DQE is a useful metric for characterizing the overall efficiency of an x-ray imaging detector. It is calculated as the square of the input SNR divided by the square of the output SNR and represents the overall detector effectiveness in producing an image with high fidelity to the incident "data" provided during acquisition. DQE ranges from 0 to 1, whereas a detector that produces information content exactly congruent to that of the x-ray beam has a DQE of 1 (this is a hypothetic situation).

CsI aSi:H FPDs are indirect x-ray conversion systems that have DQEs in the range of 0.6–0.7, superior to their direct conversion amorphous selenium (aSe) FPD competitors,

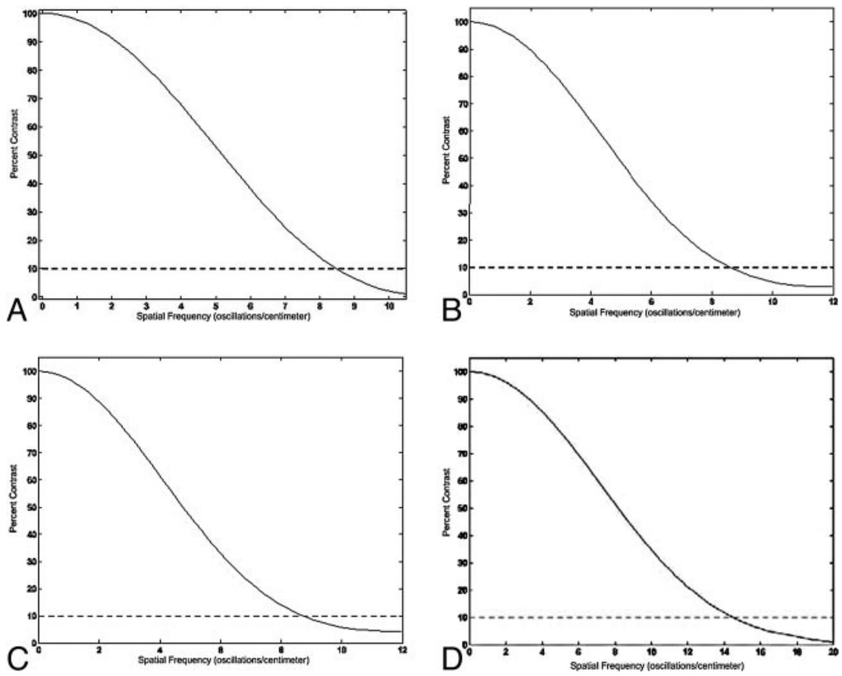

Fig 6. MTF curves for 4 MiniCAT exposure protocols. MTF curves depict spatial frequency (line pairs per centimeter) as a function of true contrast detection. Spatial resolution is conventionally described as the spatial frequency that can be discriminated with a 10% detection of true contrast. *A–D*, The MiniCAT protocols: sinus 20s 600 (20 seconds, 600 frames), sinus 10s 300 (10 seconds, 300 frames), sinus 10s 150 (10 seconds, 150 frames), and temporal bone 20s 600 (20 seconds, 600 frames) respectively. Spatial resolution is 8–9 lp/cm for the sinus 20s (600) protocol and 14–16 lp/cm for the temporal bone 20s (600) protocol. Reprinted with permission of Xoran Technologies, Ann Arbor, Mich.

which are characterized by DQEs of approximately 0.35.[26] Bacher er al[30] have demonstrated the importance of superior DQE in aSi FPDs compared with aSe detectors in a study of digital chest radiographs. Lower DQE detectors afford lower dosing during image acquisition with equal or superior clinical quality and low-contrast detectability.[30-32]

Although the introduction of high DQE indirect-conversion aSi:H FPDs into CBCT systems is a significant technical advancement, these detectors still have a slightly inferior DQE compared with the detectors traditionally used in MDCT systems.[8,33] This remains one of the technical challenges limiting low-contrast detectability in most CBCT systems.

Low-Contrast Detectability

Contrast resolution describes the ability of an imaging system to discriminate differences in tissue attenuation, as measured in HU. The low-contrast detectability in CBCT systems depends on both the dynamic range and temporal resolution of the detector as well as x-ray scatter and quantum noise.

CBCT systems under evaluation for head and neck imaging are typically described as having soft-tissue contrast discrimination of approximately 10 HU.[3,21] Modern MDCT scanners have contrast resolution approaching 1 HU. This limited contrast resolution remains a barrier to the extension of CBCT technologies into diagnostic imaging, in which detection of small changes in soft-tissue attenuation is a premium. Recent research has focused on scatter reduction and improvements in dynamic range and temporal resolution in an effort to improve contrast resolution without unnecessarily increasing patient dose. In fact, 3-HU discrimination has been achieved in experimental CBCT systems (see "Dynamic Range" subheading), though this has yet to translate to commercial scanners.[8]

Dose

The radiation-dose parameter in CT imaging is related foremost to patient safety, but it is also associated with image quality. In a simplistic model of conventional spiral CT, radiation dose increases proportionally with increased voltage (kVp) and tube current (milliampere [mA]) and can be decreased if the pixel size, section thickness, or pitch is increased. With other parameters held constant, increased radiation dose generally decreases quantum noise and affords improved contrast resolution. On the basis of the indication for imaging, exposure protocols are adapted to generate optimal image quality while delivering a justifiable dose to the patient.

An understanding of conventional CT dose measurement methodology is important to recognize the limitations confronting many CBCT dosimetry studies. By convention, the CT dose index (CTDI) and dose-length product (DLP), measured in grays (Gy), and the effective dose, measured in sieverts (Sv), are used to describe the radiation dose delivered during a CT scanning of the head or other anatomic region. Several variations on the CTDI parameter have been developed, primarily for the purposes of standardization and improved accuracy, with $CTDI_{100}$ being a common metric with defined integration limits used to describe the absorbed dose delivered during a single axial-section acquisition at particular exposure settings.[34] It is measured with a 100-mm ionization chamber implanted in a head or body phantom and is expressed as

$$\mathrm{CTDI}_{100} = \frac{1}{NT}\int_{-50mm}^{+50mm} D(z)dz,$$

where N is the number of tomographic sections imaged in a single rotation, T is the beam width, and D(z) is the dose profile function along the z-axis. The weighted CTDI ($CTDI_w$) is a more accurate reflection of the dose profile in the single-section FOV and is calculated as the weighted sum of central ($CTDI_{100c}$) and peripheral ($CTDI_{100p}$) $CTDI_{100}$s:

$$CTDI_w = (1/3)\ CTDI_{100c} + (2/3)CTDI_{100p}.$$

The DLP measures the total absorbed dose of a complete scan and is calculated by adding the $CTDI_w$ of each section in the FOV_z and then multiplying by the section thickness. The effective dose estimates a patient's stochastic risk of developing late radiation effects given the anatomic distribution of the exposure. It is calculated by multiplying absorbed dose measurements by appropriate scalars on the basis of the anatomic and physiologic characteristics of the exposure field.

Conventional dosimetry metrics such as the $CTDI_w$ cannot be directly adapted for CBCT imaging because of the altered beam geometry and scattered radiation profile of conebeam systems. Conventional ion-chamber inserts 10 cm in length do not absorb the entire expanded z-direction beam, which leads to a significant underestimation of delivered dose.[18,35,36] Attempts have been made to develop techniques that generate absorbed-dose metrics comparable with those used in conventional CT, such as the $CTDI_w$, but a standardized and universally applicable technique has yet to be adopted.[8,18,36] Viewed collectively, dosing studies of head and neck CBCT scans also have a lack of common exposure protocols and measurement methodologies, producing a wide range of results and making it difficult to draw coherent overall conclusions.[8]

Accurate dose evaluation is important for CBCT technology because these systems are often touted as low-dose alternatives to MDCT for applications such as sinus and temporal bone imaging, among others. Most dosimetry experiments suggest that the dose delivered during CBCT scans is lower than that in conventional MDCT for similar imaging studies, but it has been difficult to control the many variables affecting radiation dose. There is speculation that there may actually be little difference in absorbed dose measurements when FOVs and image quality parameters between CBCT and MDCT are approximated.[8,18,37]

Commercial CBCT scanners designed for dedicated head and neck imaging have application-specific exposure parameter protocols, with FOVs designed to capture the area of interest and minimize exposure to adjacent structures. In the absence of a standardized absorbed dose metric comparable with the CTDI used in conventional CT, estimations of an effective dose for these scanners are often evaluated by point-dose measurements generated with thermoluminescent devices implanted into anthropomorphic head phantoms. In an experimental C-arm model, Daly et al[38] found the effective dose for a head and neck CBCT scan of 16-cm head phantoms to be 0.1–0.35 mSv, depending on whether exposure parameters were optimized for bony or soft-tissue resolution. For reference, the expected effective dose of a typical MDCT scan of the head is 1–2 mSv.[34] An effective dose for sinus imaging in commercial dedicated head and neck CBCT scanners has been estimated to be approximately 0.2 mSv.[39,40] Peltonen et al[37] described the effective dose for limited CBCT imaging of the middle ear to be 13 uSv, 60 times lower than that of a conventional MDCT scan of the temporal bone.

Comparisons of point-dose measurements have also been made for commercial dedicated dentomaxillofacial CBCT scanners, yielding effective dosing in the range of 13–498 μSv, most falling in the approximate range of 30–80 μSv, depending on scanning protocol, FOV, and manufacturer.[41-43]

Conclusions

CBCT is an emerging technical advancement in CT imaging that uses a conebeam acquisition geometry and FPD to provide relatively low-dose imaging with high isotropic spatial resolution acquired with a single gantry revolution. Efficient use of the x-ray beam in CBCT imaging produces a relatively low x-ray tube power requirement, which, along with flat panel detection and limited anatomic coverage, has facilitated the production of compact CBCT scanners suitable for use in an office-based setting. CBCT acquisition parameters can be optimized to produce isometric voxels as small as a $150 \times 150 \times 150\ \mu m^3$ at the isocenter. Limited contrast resolution, however, continues to impair low-contrast detectability in CBCT images. Several factors contribute to this limited contrast resolution, including the increased x-ray scatter in conebeam acquisition, the lower DQE of CBCT systems compared with MDCT, and the limited temporal range of aSi:H FPDs. Improvements in scatter subtraction methods continue to be the subject of research aimed at improving image quality in CBCT systems. Dedicated CBCT scanning of restricted anatomic volumes in the maxillofacial region can be obtained with effective patient dosing in the approximate range of 30–80 μSv, and imaging of the paranasal sinuses is possible with delivery of ~0.2 mSv. Research on patient dose, however, has been conducted with largely variable exposure parameters and still requires further research and adoption of an appropriate dose metric for comparison with MDCT scanning.

Acknowledgments

We thank Karen Carter for help with image preparation, Xoran Technologies for their provision of graphics and technical data, and Sylvia Miracle for her review of the manuscript.

References

1. Robb RA. **The dynamic spatial reconstructor: an x-ray video-fluoroscopic CT scanner for dynamic volume imaging of moving organs.** *IEEE Trans Med Imaging* 1982;1:22–33
2. Orth RC, Wallace MJ, Kuo MD, for the Technology Assessment Committee of the Society of Interventional Radiology. **C-arm cone-beam CT: general principles and technical considerations for use in interventional radiology**. *J Vasc Interv Radiol* 2008;19:814–20. Epub 2008 Apr 23
3. Dörfler A, Struffert T, Engelhorn T, et al. **Rotational flat-panel computed tomography in diagnostic and interventional neuroradiology.** *Rofo* 2008;180:891–98
4. Moore CJ, Am A, Marchant T, et al. **Developments in and experience of kilovoltage x-ray cone beam image-guided radiotherapy.** *Br J Radiol* 2006;79(Spec No 1):S66–78
5. Hounsfield GN. **Nobel Award address: computed medical imaging.** *Med Phys* 1980;7:283–90
6. Seeram E. *Computed Tomography: Physical Principles, Clinical Applications, and Quality Control.* Philadelphia: W.B. Saunders; 2001:2–3
7. Scarfe WC, Farman AG, Sukovic P. **Clinical applications of cone-beam computed tomography in dental practice.** *J Can Dent Assoc* 2006;72:75–80
8. Gupta R, Grasruck M, Suess C, et al. **Ultra-high resolution flat-panel volume CT: fundamental principles, design architecture, and system characterization.** *Eur Radiol* 2006;16:1191–205. Epub 2006 Mar 10
9. Baba R, Konno Y, Ueda K, et al. **Comparison of flat-panel detector and image-intensifier detector for cone-beam CT.** *Comput Med Imaging Graph* 2002;26:153–58
10. Feldkamp LA, Davis LC, Kress JW. **Practical cone-beam algorithm.** *J Opt Soc Am* 1984;A1:612–19

11. Yan XH, Leahy RM. **Derivation and analysis of a filtered backprojection algorithm for cone beam projection data.** *IEEE Trans Med Imaging* 1991;10:462–72
12. Kudo H, Noo F, Defrise M, et al. **New super-short-scan algorithm for fan-beam and cone-beam reconstruction.** *IEEE NSS-MIC* 2002;902–06
13. Gupta R, Bartling SH, Basu SK, et al. **Experimental flat-panel high-spatial-resolution volume CT of the temporal bone.** *AJNR Am J Neuroradiol* 2004;25:1417–24
14. Siewerdsen JH, Jaffray DA. **Cone-beam computed tomography with a flat-panel imager: magnitude and effects of x-ray scatter.** *Med Phys* 2001;28:220–31
15. Graham SA, Moseley DJ, Siewerdsen JH, et al. **Compensators for dose and scatter management in cone-beam computed tomography.** *Med Phys* 2007;34:2691–703
16. Siewerdsen JH, Moseley DJ, Bakhtiar B, et al. **The influence of antiscatter grids on soft-tissue detectability in cone-beam computed tomography with flat-panel detectors.** *Med Phys* 2004;31:3506–20
17. Ning R, Chen B, Yu R, et al. **Flat panel detector-based cone-beam volume CT angiography imaging: system evaluation.** *IEEE Trans Med Imaging* 2000;19:949–63
18. Fahrig R, Dixon R, Payne T, et al. **Dose and image quality for a cone-beam C-arm CT system.** *Med Phys* 2006;33:4541–50
19. Neitzel U. **Grids or air gaps for scatter reduction in digital radiography: a model calculation.** *Med Phys* 1992;19:475–81
20. Nickoloff EL, Lu ZF, Dutta A, et al. **Influence of flat-panel fluoroscopic equipment variables on cardiac radiation doses.** *Cardiovasc Intervent Radiol* 2007;30:169–76
21. Wiegert J, Bertram M, Schafer D, et al. **Soft tissue contrast resolution within the head of human cadaver by means of flat detector based cone-beam CT.** *Proc SPIE* 2004;5368:330–37
22. Jarry G, Graham SA, Moseley DJ, et al. **Characterization of scattered radiation in kV CBCT images using Monte Carlo simulations.** *Med Phys* 2006;33:4320–29
23. Siewerdsen JH, Daly MJ, Bakhtiar B, et al. **A simple, direct method for x-ray scatter estimation and correction in digital radiography and cone-beam CT.** *Med Phys* 2006;33:187–97
24. Ning R, Tang X, Conover D. **X-ray scatter correction algorithm for cone beam CT imaging.** *Med Phys* 2004;31:1195–202
25. Malusek A, Sandborg M, Carlsson GA. **Simulation of scatter in cone beam CT: effect on projection image quality.** *Proc SPIE* 2003;5030:740–51
26. Cowen AR, Kengyelics SM, Davies AG. **Solid-state, flat-panel, digital radiography detectors and their physical imaging characteristics.** *Clin Radiol* 2008;63:487–98. Epub 2008 Jan 31
27. Roos PG, Colbeth RE, Mollov I, et al. **Multiple gain ranging readout method to extend the dynamic range of amorphous silicon flat panel imagers.** *Proc SPIE* 2004;5368:139–49
28. Akpek S, Brunner T, Benndorf G, et al. **Three-dimensional imaging and cone beam volume CT in C-arm angiography with flat panel detector.** *Diagn Interv Radiol* 2005;11:10–13
29. Cowen AR, Davies AG, Sivananthan MU. **The design and imaging characteristics of dynamic, solid-state, flat-panel x-ray image detectors for digital fluoroscopy and fluorography.** *Clin Radiol* 2008;63:1073–85
30. Bacher K, Smeets P, Vereecken L, et al. **Image quality and radiation dose on digital chest imaging: comparison of amorphous silicon and amorphous selenium flat-panel systems.** *AJR Am J Roentgenol* 2006;187:630–37
31. Bacher K, Smeets P, Bonnarens K, et al. **Dose reduction in patients undergoing chest imaging: digital amorphous silicon flat-panel detector radiography versus conventional film-screen radiography and phosphor-based computed radiography.** *AJR Am J Roentgenol* 2003;181:923–39
32. Völk M, Paetzel C, Angele P, et al. **Routine skeleton radiography using a flat-panel detector: image quality and clinical acceptance at 50% dose reduction.** *Invest Radiol* 2003;38:230–35
33. Farman TT, Vandre RH, Pajak JC, et al. **Effects of scintillator on the detective quantum efficiency (DQE) of a digital imaging system.** *Oral Surg Oral Med Oral Pathol Oral Radiol Endod* 2006;101:219–23. Epub 2005 Nov 11
34. Bauhs JA, Vrieze TJ, Primak AN, et al. **CT dosimetry: comparison of measurement techniques and devices.** *Radiographics* 2008;28:245–53
35. Mori S, Endo M, Nishizawa K, et al. **Enlarged longitudinal dose profiles in cone-beam CT and the need for modified dosimetry.** *Med Phys* 2005;32:1061–69
36. Kyriakou Y, Deak P, Langner O, et al. **Concepts for dose determination in flat-detector CT.** *Phys Med Biol* 2008;53:3551–66. Epub 2008 Jun 13
37. Peltonen LI, Aarnisalo AA, Kortesniemi MK, et al. **Limited cone-beam computed tomography imaging of the middle ear: a comparison with multislice helical computed tomography.** *Acta Radiol* 2007;48:207–12
38. Daly MJ, Siewerdsen JH, Moseley DJ, et al. **Intraoperative cone-beam CT for guidance of head and neck surgery: assessment of dose and image quality using a C-arm prototype.** *Med Phys* 2006;33:3767–80
39. Jackman AH, Palmer JN, Chiu AG, et al. **Use of intraoperative CT scanning in endoscopic sinus surgery: a preliminary report.** *Am J Rhinol* 2008;22:170–74
40. Alspaugh J, Christodoulou E, Goodsitt M, et al. **Dose and image quality of flat-panel detector volume computed tomography for sinus imaging.** *Med Phys* 2007;34:2634
41. Silva MA, Wolf U, Heinicke F, et al. **Cone-beam computed tomography for routine orthodontic treatment planning: a radiation dose evaluation.** *Am J Orthod Dentofacial Orthop* 2008;133:640.e1–5
42. Loubele, M, Bogaerts R, Van Dijck E, et al. **Comparison between effective radiation dose of CBCT and MSCT scanners for dentomaxillofacial applications.** *Eur J Radiol* 2008 Jul 16. [Epub ahead of print]
43. Ludlow JB, Ivanovic M. **Comparative dosimetry of dental CBCT devices and 64-slice CT for oral and maxillofacial radiology**. *Oral Surg Oral Med Oral Pathol Oral Radiol Endod.* 2008;106:106–14. Epub 2008 May 27

Attachment D

REVIEW ARTICLE

Conebeam CT of the Head and Neck, Part 2: Clinical Applications

A.C. Miracle
S.K. Mukherji

SUMMARY: Conebeam x-ray CT (CBCT) is being increasingly used for point-of-service head and neck and dentomaxillofacial imaging. This technique provides relatively high isotropic spatial resolution of osseous structures with a reduced radiation dose compared with conventional CT scans. In this second installment in a 2-part review, the clinical applications in the dentomaxillofacial and head and neck regions will be explored, with particular emphasis on diagnostic imaging of the sinuses, temporal bone, and craniofacial structures. Several controversies surrounding the emergence of CBCT technology will also be addressed.

Conebeam CT (CBCT) is an advancement in CT imaging that has begun to emerge as a potentially low-dose cross-sectional technique for visualizing bony structures in the head and neck. The physical principles, image quality parameters, and technical limitations relevant to CBCT imaging were discussed in Part 1 of this 2-part series. The second part presented here will highlight the evidence related to CBCT applications in head and neck as well as dentomaxillofacial imaging. Controversial aspects of this technology will also be addressed, including limitations in image quality and its often office-based operational model.

CBCT was first adapted for potential clinical use in 1982 at the Mayo Clinic Biodynamics Research Laboratory.[1] Initial interest focused primarily on applications in angiography in which soft-tissue resolution could be sacrificed in favor of high temporal and spatial-resolving capabilities. Since that time, several CBCT systems have been developed for use both in the interventional suite and for general applications in CT angiography.[2,3] Exploration of CBCT technologies for use in radiation therapy guidance began in 1992,[4,5] followed by integration of the first CBCT imaging system into the gantry of a linear accelerator in 1999.[6]

The first CBCT system became commercially available for dentomaxillofacial imaging in 2001 (NewTom QR DVT 9000; Quantitative Radiology, Verona, Italy). Comparatively low dosing requirements and a relatively compact design have also led to intense interest in surgical planning and intraoperative CBCT applications, particularly in the head and neck but also in spinal, thoracic, abdominal, and orthopedic procedures.[7-11] Diagnostic applications in CT mammography and head and neck imaging are also under evaluation.[12-14] The technical and clinical considerations pertaining to CBCT imaging in many of these applications have been the subjects of several recent reviews.[15-19] The recent review by Dörfler et al[16] of the neurointerventional applications of CBCT is of particular interest to the field of neuroradiology.

The discussion below will focus on the diagnostic and treatment-planning applications of CBCT in dentomaxillofacial and head and neck imaging. Commercially available CBCT systems for dentomaxillofacial imaging include the CB MercuRay and CB Throne (Hitachi Medical, Kashiwi-shi, Chiba-ken, Japan), 3D Accuitomo products (J. Morita Manufacturing, Kyoto, Japan), and iCAT (Xoran Technologies, Ann Arbor, Mich; and Imaging Sciences International, Hatfield, Pa). Similar systems designed for point-of-service head and neck imaging have also recently become available (MiniCAT, Xoran Technologies; 3D Accuitomo and 3D Accuitomo 170, J Morita Manufacturing; ILUMA Cone Beam CT, IMTEC, Ardmore, Okla and GE Healthcare, Chalfont St. Giles, UK).

From the Departments of Radiology (A.C.M., S.K.M.), Otolaryngology (S.K.M.), and Radiation Oncology (S.K.M.), University of Michigan Health System, University Hospital, Ann Arbor, Mich.

Please address correspondence to Aaron Miracle, University of Michigan Medical Center, Department of Radiology, B2B311 UH SPC 5030, 1500 East Medical Center Dr, Ann Arbor, MI 48109-5030; e-mail: amiracle@med.umich.edu

Indicates open access to non-subscribers at www.ajnr.org

DOI 10.3174/ajnr.A1654

Dentomaxillofacial Imaging

Advanced cross-sectional imaging techniques such as CT are used in dentomaxillofacial imaging to solve complex diagnostic and treatment-planning problems, such as those encountered in craniofacial fractures, endosseous dental-implant planning, and orthodontics, among others. With the advent of CBCT technology, cross-sectional imaging that had previously been outsourced to medical CT scanners has begun to take place in dental offices.

Early dedicated CBCT scanners for dental use were characterized by Mozzo et al[20] and Arai et al[21] in the late 1990s. Since then, more commercial models have become available, inciting research in many fields of dentistry and oral and maxillofacial surgery. To date, multiple ex vivo studies have attempted to establish the ability of CBCT images to accurately reproduce the geometric dimensions of the maxillodental structures and the mandible.[22-25]

A relatively low patient dose for dedicated dentomaxillofacial scans is a potentially attractive feature of CBCT imaging. The dosing characteristics of dentomaxillofacial scanners were discussed in Part 1 of this series. An effective dose in the broad range of 13–498 μSv can be expected, with most scans falling between 30 and 80 μSv, depending on exposure parameters and the selected FOV size. In comparison, standard panoramic radiography delivers ~13.3 μSv and multidetector CT with a similar FOV delivers ~860 μSv.[26,27] Image quality can vary considerably with dose; images acquired with higher radiation exposure often produce superior image quality.

The discussion below reviews potential CBCT applications in the dentomaxillofacial regions. Most of this research remains preliminary; further prospective and outcomes-based research is required to make informed recommendations on the appropriate use of CBCT in dentomaxillofacial imaging.

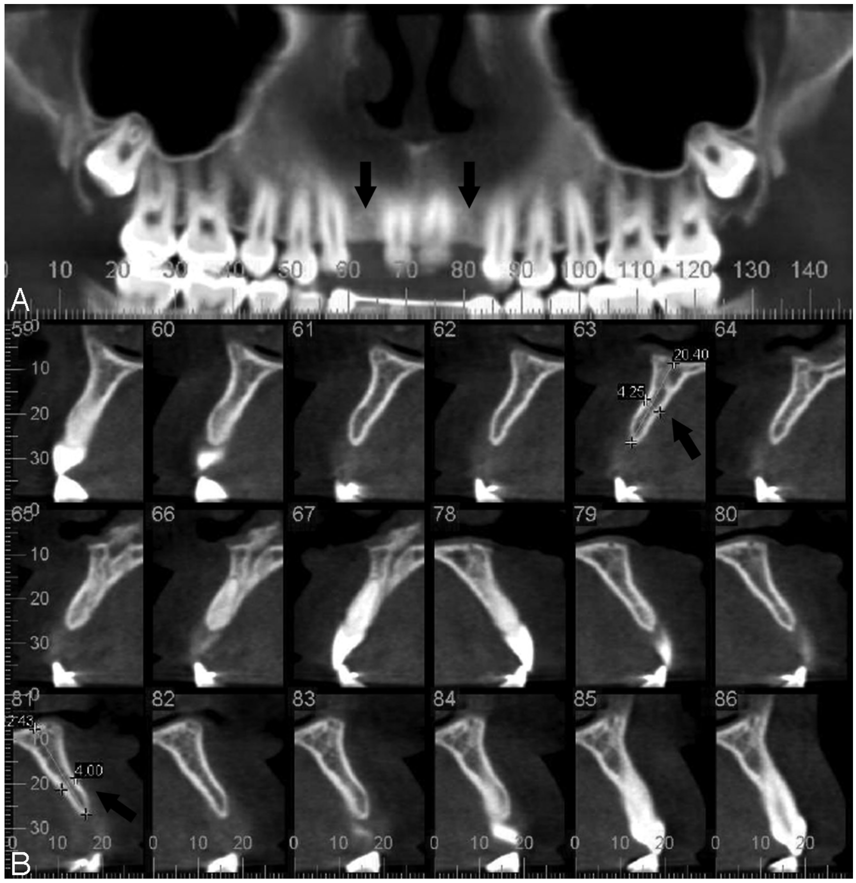

Fig 1. Noncontrast dentomaxillofacial CBCT scan (iCAT) of a patient with congenital absence of the maxillary lateral incisors (0.4-mm pixels, 120 kVp, 18.66 mA). *A*, Reconstructed panoramic view of the maxilla demonstrates bilateral lateral incisor absence (*arrows*). *B*, Sequential parasagittal/oblique views through the maxillary alveolar bone demonstrate planned implant locations (*arrows*).

Implantology

Cross-sectional imaging techniques can be an invaluable tool during preoperative planning for complicated endosseous dental implantation procedures.[28] Conventional linear tomography and CT have traditionally been used in presurgical imaging, though the former has overlain ghosting artifacts and the latter has relatively high radiation exposure and cost.[29]

Practitioners have begun using office-based CBCT scanners in preoperative imaging for implant procedures, capitalizing on availability and low dosing requirements. A review by Guerrero et al[30] outlines the clinical and technical aspects of CBCT, which have popularized this new technique. Preliminary evidence addresses the ability of CBCT images to characterize mandibular and alveolar bone morphology, as well as to visualize the maxillary sinuses, incisive canal, mandibular canal, and mental foramina, all structures particularly important in surgical planning for dental implantation.[29,31,32] Several studies have described the 3D geometric accuracy of CBCT imaging in the maxillodental and mandibular regions as well.[22-25] Examples of CBCT imaging studies for implant planning and visualization of the mandibular canal are presented in Figures 1 and 2 respectively.

Craniofacial Fractures

Imaging of complex high-contrast bony structural pathology such as craniofacial fractures is a logical application for CBCT. Terakado et al[33] reported a case series in 2000, which included 2 patients with facial trauma for whom CBCT was used to characterize a mandibular head fracture, dental root fractures, and the displacement of anterior maxillary teeth. Since that time, several additional reports have extolled the low-dose high-resolution properties of CBCT imaging in preoperative characterization of mandibular and orbital floor fractures.[34-36] In orbital floor fractures, although CBCT can demonstrate orbital content herniation, it lacks the contrast resolution to differentiate the tissue composition of the herniated materials.[35]

The intraoperative uses of C-arm CBCT systems have been evaluated for fractures of the zygomaticomaxillary complex (ZMC), demonstrating the feasibility of CBCT use in surgical navigation, localization of bony fragments, and evaluation of screw anchorage and plate fittings with low levels of metal artifact.[37,38] These results have been corroborated in a study of postoperative patients with ZMC fractures, though investigators noted that poorly aerated ethmoidal air cells limit the ability of CBCT to visualize the medial orbital wall.[39] Low bone density in older patients also reduced bony structural definition in their series. Intraoperative efficacy has been evaluated in mandibular fracture fixation as well.[40]

Orthodontics

Cross-sectional imaging affords overlay-free visualization of structural and anatomic relationships important for addressing many radiologic questions in orthodontics. The current

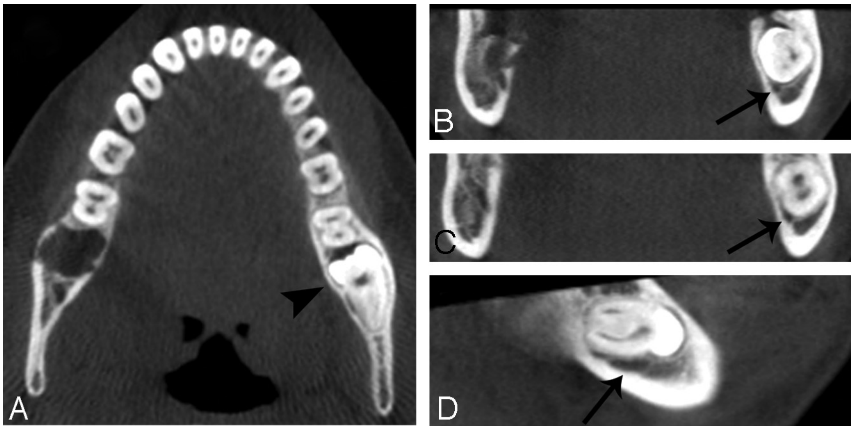

Fig 2. Noncontrast dentomaxillofacial CBCT scan (iCAT) of a patient with an impacted left mandibular third molar (0.4-mm pixels, 120 kVp, 18.66 mA). *A*, Axial view through the mandible demonstrates the impacted molar on the left side (*arrowhead*). *B*–*D*, Coronal (*B* and *C*) and sagittal (*D*) views through the mandibular body depict the proximity of the underlying mandibular canal (*arrows*) to the impacted molar.

Fig 3. Noncontrast CBCT scan of a 56-year-old acquired with a sinus protocol (40 seconds, 600 frames, 0.4-mm pixels, 120 kVp, 48 mA). *A*, Axial section demonstrates right-sided deviation of the nasal septum and mucosal thickening in the left nasal cavity. *B*, Coronal section redemonstrates mucosal thickening of the left nasal cavity. *C*, Left paramedian sagittal section. *D*, Axial view of the ethmoid air cells and sphenoid sinus with mild opacification in the region of the right sphenoethmoidal recess.

standard of care for overlay-free imaging in orthodontics is conventional CT.[41] Low-cost office-based CBCT imaging has recently been explored for orthodontic applications, including assessment of palatal bone thickness, skeletal growth patterns, dental age estimation, upper airway evaluation, and visualization of impacted teeth.[42-47] Although preliminary results are encouraging, established cross-sectional techniques such as conventional CT provide superior image quality of dental and surrounding structures for advanced orthodontic treatment planning.[41] Low dosing requirements appear to remain a benefit of CBCT when compared with conventional CT, with a routine orthodontic CBCT study delivering an effective dose of ≤61.1 μSv compared with 429.7 μSv for multisection CT.[48] Lateral cephalograms deliver 10.4 μSv in comparison, though without the benefit of 3D structural visualization.

Temporomandibular Joint

Morphologic changes of the temporomandibular joint (TMJ) as depicted with conventional MR imaging, CT, and radiographic imaging are often useful in diagnosing pathologic

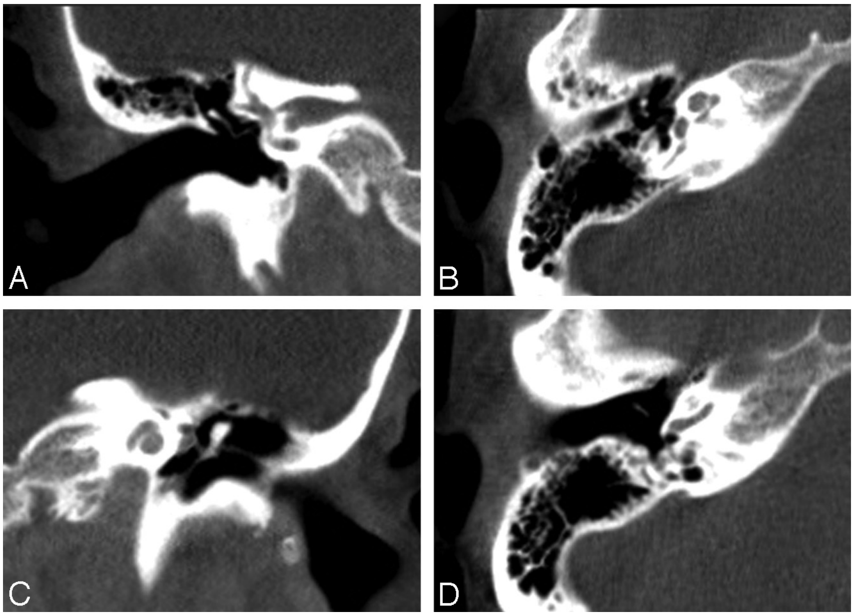

Fig 4. Noncontrast CBCT scan of a 50-year-old acquired with a temporal bone protocol (40 seconds, 600 frames, 0.3-mm-pixels, 125 kVp, 50.85 mA). *A*, Coronal image of the normal right temporal bone demonstrates the vestibulocochlear nerve, body and long limb of the incus, as well as the stapedial neck and crura in the fossa of the oval window. *B*, Axial section at the level of the right mesotympanum demonstrates the head of the malleus, short limb of the incus, and stapedial crura, as well as the cochlear nerve, tensor tympani, and mastoid part of the facial nerve VII. *C*, Coronal section through the left cochlea demonstrates the modiolus, tympanic part of facial nerve VII, tensor tympani, and malleus. *D*, Axial section through the right mesotympanum at the level of the round window demonstrates the handle of the malleus, base of cochlea, and mastoid portion of the facial nerve VII.

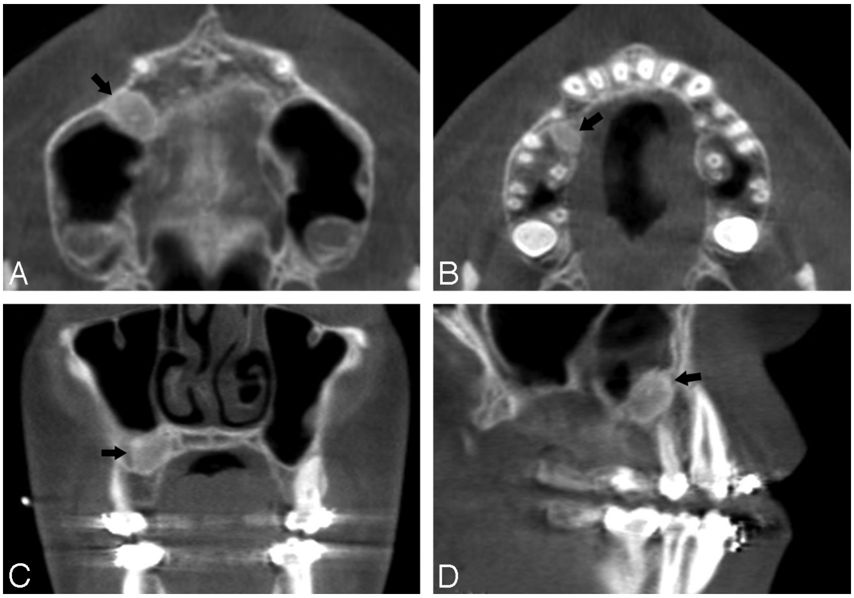

Fig 5. Noncontrast CBCT scan of a 13-year-old boy acquired with a sinus protocol (40 seconds, 600 frames, 0.4-mm pixels, 120 kVp, 48 mA). *A*, Axial section at the level of the maxillary sinus floor demonstrates a 1.0 × 0.7 × 1.0-cm oval mass in the alveolar process of the right maxilla (*arrow*). *B*, Axial image highlights the inferior extent of the lesion in *A*. *C* and *D*, Coronal and sagittal images, respectively, of the lesion in *A*.

processes such as degenerative changes and ankylosis, joint remodeling after diskectomy, malocclusion, and congenital and developmental malformations.[49] CBCT is a technique that has recently inspired research in TMJ imaging, though preliminary experiments have yet to translate into clinical studies. Several cadaveric series have explored the use of TMJ CBCT to assess periarticular bony defects, flattenings, osteophytes, and sclerotic changes.[50-53] Preliminary studies have also directly compared CBCT with radiography, multidetector row CT (MDCT), and linear tomography for detection of osseous abnormalities of the TMJ.[52,53] Although early results are promising, more research is needed before CBCT should be used clinically to assess the TMJ. A recent systematic review by Hussain et al[54] suggests that axially corrected sagittal tomography is still the method of choice in the detection of periarticular erosions and osteophytes.

Endodontics

CBCT has been explored for applications in endodontics, including periradicular surgical planning, assessment of periapical pathology, and dentoalveolar trauma evaluation.[55] The diagnostic properties of CBCT at the root apices and perira-

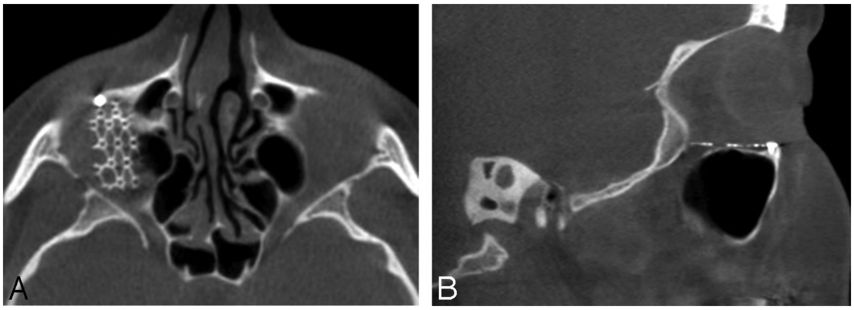

Fig 6. Noncontrast CBCT scan of a 45-year-old (40 seconds, 600 frames, 0.4-mm pixels, 120 kVp, 48 mA) obtained after repair of a right orbital floor fracture. *A*, Axial image demonstrates a metal fixture implanted over the right orbital floor. *B*, Metallic implant is seen in the sagittal section.

dicular region have been reported in several studies.[56-58] In retrospective cohorts and case reports, CBCT has been suggested as superior to periapical radiographs in the characterization of periapical lucent lesions, reliably demonstrating lesion proximity to the maxillary sinus, sinus membrane involvement, and lesion location relative to the mandibular canal.[56-58] There may also eventually be a role for CBCT in early detection of periapical disease, which could lead to better endodontic treatment outcomes.[55] Promising results have been demonstrated in studies characterizing CBCT images for endodontic surgical planning purposes as well.[58,59]

Periodontics

The first reported applications of CBCT in periodontology were for diagnostic and treatment-outcome evaluations of periodontitis.[60] Ex vivo studies later characterized the ability of CBCT to accurately reconstruct periodontal intrabony and fenestration defects, dehiscences, and root furcation involvements in comparison with radiography, MDCT, and histologic measurements.[61-65] CBCT 3D geometric accuracy has been suggested to be equal to radiography and MDCT but with better observer-rated image quality than MDCT as well as superior periodontal-defect detection than radiography.[61,62,64] Although periodontal bony defects are well visualized with CBCT, conventional radiography still affords higher quality bony contrast and delineation of the lamina dura.[63] CBCT ex vivo visualization of the periodontal ligament and periodontal ligament space has been evaluated in comparison with radiography with mixed results, a more recent study suggesting that CBCT visualization is still inferior to that of radiography.[61,66]

Head and Neck

As CBCT imaging systems have become more widely available, interest in the intraoperative and diagnostic CBCT applications in the extracranial head and neck regions has intensified. The reported high isotropic spatial resolution and relatively low dose requirements of CBCT are characteristics that have made it particularly attractive. In the head and neck region, a premium is placed on discriminating fine anatomic detail in territories where the vascular and bony structural anatomy is particularly complex.[8] Potential applications in sinus, temporal bone, and skull base imaging have been explored, as discussed below. Figures 3, 4, 5, and 6 depict head and neck CBCT studies visualizing the paranasal sinuses; temporal bones; maxillary sinus floor and alveolar process of the maxilla; and orbital floors respectively.

Sinus Imaging/Frontal Recess

Comparatively low dosing requirements, high-quality bony definition, and the compact design afforded by CBCT scanners have made them attractive for office-based and intraoperative scanning of the paranasal sinuses.[67,68] To date, there have been few studies comparing image quality in paranasal sinus CBCT scans with that in MDCT. Alspaugh et al[69] did directly compare the spatial resolution obtained with CBCT scans of the paranasal sinuses with that of 16- and 64-section MDCT scanners. They concluded that 12 line pairs per centimeter (lp/cm) isotropic spatial resolution could be obtained with an effective dose of 0.17 mSv compared with a dose requirement of 0.87 mSv for 11-lp/cm spatial resolution in a 64-section MDCT scanner.

To a large degree, evidence supporting sinus CBCT imaging has emerged from exploration of intraoperative CBCT applications in endoscopic sinus surgery (ESS). In preclinical cadaver studies, Rafferty et al[67] provided proof of principle for the application of C-arm CBCT imaging to ESS, concluding that both spatial and soft-tissue contrast was sufficient to aid surgical navigation in the frontal recess. More recent clinical studies have also provided qualitative evidence that intraoperative CBCT provides high-quality definition of bony anatomy, which can lead to refinement of surgical strategy.[70,71] In a series of 25 patients undergoing ESS, Batra et al[71] found that residual bony partitions and stent locations could be visualized with intraoperative CBCT scans, leading to surgical revision. CBCT has also been used recently to evaluate contrast delivery during sinus irrigation after ESS.[72]

Preliminary evidence suggests that CBCT may be suited for specific imaging tasks in the context of intraoperative and perioperative bony structural evaluations, enabling low-dose assessment of individualized paranasal sinus anatomy, surgical outcomes, and stent placements. To our knowledge, there is no current evidence, however, supporting CBCT use in general diagnostic sinus imaging owing to lack of soft-tissue contrast resolution. Furthermore, significant complications of ESS, including encephalocele, subarachnoid hemorrhage, and meningitis are unlikely to be evaluated adequately with current CBCT image quality.[73,74]

Temporal Bone/Lateral Skull Base

The temporal bone was one of the earliest targets for head and neck CBCT imaging. Specific applications have been explored, including postprocedural middle and inner ear implant evaluation, visualization of the reuniting duct in the inner ear, and intraoperative temporal bone surgical guidance.[8,75,76]

Preliminary evaluation of an experimental CBCT system for general temporal bone diagnostic imaging was performed by Gupta et al[12] on a small series of partially manipulated cadaveric specimens. They found that observer scores of the quality of structural visualization with CBCT were significantly higher compared with scores for MDCT. Particularly well-visualized structures included the ossicular chain, bony labyrinth of the inner ear, internal cochlear anatomy, and the facial nerve. They also noted reduced metal artifacts with cochlear implant imaging as well as improved detection of small laser-induced lesions in the ossicular chain. Gupta et al suggest that lack of soft-tissue contrast in their evaluations did not interfere with diagnostic accuracy due to the abundance of high-contrast structures housed in the temporal bone and the positive effect of higher spatial resolution on resolving some low-contrast structures such as the facial nerve.

Peltonen et al[14] compared a commercially available CBCT scanner with MDCT in a study on unoperated temporal bone specimens by using a modified Likert scale (scored by 2 otologists and 1 radiologist) to assess visualization of important structures in the lateral skull base. They concluded that CBCT was at least as accurate as MDCT in defining surgically relevant middle ear structures. The inner ear was incompletely visualized with CBCT in their study.

Perhaps the most well-studied use of temporal bone CBCT is for the evaluation of middle and inner ear implants. Early preclinical studies in temporal bone specimens fitted with cochlear implants demonstrated that an adapted CT angiography CBCT system could noninvasively depict the electrode-modiolus relationship postimplantation.[77,78] These results were later corroborated in another cadaver study comparing single- and multisection CT with CBCT.[79] When compared with single- or multisection CT, a reduction in metal artifacts was observed with CBCT, which allowed more precise determination of electrode-array positioning within the scala tympani or scala vestibuli.[79] Reduced metal artifacts with implant imaging using CBCT compared with conventional CT were also demonstrated by Offergeld et al[80] in a study evaluating middle ear implants in postsurgical temporal bone specimens.

Preclinical studies have been followed by studies of patients with inner and middle ear implants, suggesting that the combination of high spatial resolution and reduced metal artifacts with CBCT imaging may facilitate the postsurgical evaluation of reconstructed middle and inner ears.[75,81] A recent study has also explored the utility of CBCT in evaluating progressive hearing loss. Dalchow et al[82] submitted 25 patients with audiometry-confirmed conductive hearing loss to preoperative CBCT and concluded that CBCT could be accurate both in predicting the continuity of the ossicular chain and in detecting ossicular erosions.

Multiple commercial CBCT systems have temporal bone−acquisition protocols. The miniCAT acquires temporal bone images at 125 kilovolt (peak) (kVp) and 58.8 mA with a 20-second scanning time using a sharp kernel (manufacturer's data). This protocol delivers 4.62 and 4.18 mGy at the center and periphery, respectively, of a 100-mm ion chamber, achieving spatial resolution in the range of 14–16 lp/cm (manufacturer's data). In their study of limited-FOV temporal bone imaging described above, Peltonen et al[14] noted a 60-fold effective dose reduction with CBCT compared with MDCT, though they attributed much of this dramatic reduction to significantly smaller FOVs and shorter scanning times for their CBCT images. They noted that low-dose MDCT settings can acquire images with effective doses like those in CBCT if the FOVs and scanning times are, in fact, comparable with those of CBCT.[14]

These data suggest that CBCT might be useful for select imaging tasks in temporal bone imaging, including evaluation of inner and middle ear implant positioning, as well as definition of high-contrast postsurgical change and structural anatomy within the lateral skull base. Possible applications in evaluation of bony pathology, such as ossicular chain erosions, may also be emerging. Currently, further research is required to characterize the ability of CBCT to define temporal bone structures and bony pathology reliably, especially given the technologic and scan-parameter variability of commercial CBCT scanners. Lack of soft-tissue contrast resolution also continues to limit the use of CBCT in general diagnostic imaging of the temporal bone.

Skull Base

The particularly complex bony and neurovascular anatomy of the skull base makes it an attractive target for high-spatial-resolution imaging. Current practices in oncologic imaging of the skull base rely on MDCT and MR imaging for combined osseous and soft-tissue definitions.[83] Several preclinical reports have begun to explore the potential uses of CBCT during surgeries at the skull base,[7,84,85] suggesting high 3D localization accuracy and low target-registration error with effective doses in the range of 0.1–0.35 mSv. The xCAT intraoperative CBCT scanner (Xoran Technologies), a cousin of the MiniCat, has been evaluated in clinical scenarios at the skull base as well, with favorable preliminary results.[71,86]

Controversies

As with any emerging imaging technology, use of CBCT scanners has been the subject of criticism as well as acclaim. The technology itself is limited by lack of user experience and what is currently a relatively small body of related literature. The point-of-service operational model that dominates diagnostic head and neck CBCT imaging practices has also drawn criticism. Additionally, the *ACR Practice Guideline* for CT of the head and neck recommends that all imaging studies be evaluated with bone and soft-tissue algorithms.[87] Because of the low radiation dose, CBCT can only provide bony detail and is unable to provide images of the soft tissues.

At our institution, CBCT scanning of the extracranial head and neck is performed in both a clinical and research capacity primarily for sinus, maxillofacial, and occasional temporal bone imaging. Research on this technology is still preliminary, without prospective studies that convincingly demonstrate its benefit compared with conventional CT.

Both in medical and oral and maxillofacial imaging in dentistry, CBCT has been largely adopted as an office-based service. This is a usage model purported to expedite patient diagnosis and treatment while simultaneously reducing costs, providing 1-stop management with fewer billed visits and no radiologist consultation fees. Point-of-service imaging and other self-referral services, however, have been widely criticized for encouraging overuse and directly inflating medical costs.

The belief that financial incentives undermine the clinical decision-making process has been the basis for federal legislation limiting Medicare payments for self-referral services (so-called "Stark laws"). Regulatory checks on the operation of imaging technologies are present in many states in the form of Certificates of Need (CONs), which require documentation of sufficient community demand before a technology can be certified to be operated at a particular facility. This theoretically prevents excess capacity of medical equipment and prevents cost inflation. In states with CON laws, CBCT scanners are often treated like conventional CT scanners and are subject to the same scanning-volume requirements regulating the acquisition and operation of conventional CT scanners. The CT allowance in a given community is typically filled by conventional scanners, making it difficult to operate a CBCT machine in states with CON laws.

The advent of CBCT technologies has also fueled the controversy surrounding office-based imaging, which is usually performed and interpreted by nonradiologists often without the accreditation, training, or licensure afforded by the radiology community. A recent position paper by the American Academy of Oral and Maxillofacial Radiology addressed this issue, emphasizing the role of the practitioner in obtaining and interpreting CBCT images. It highlights the practitioner's responsibility for understanding CBCT operating parameters, reviewing the entire exposed tissue volume, and addressing all radiologic findings irrespective of their association with the scanning indication.[88]

Conclusions

CBCT is an emerging CT technology, which has potential applications for imaging of high-contrast structures in the head and neck as well as dentomaxillofacial regions. Preliminary research suggests that high-spatial-resolution images can be obtained with comparatively low patient dose. To date, the most researched applications for head and neck CBCT are in sinus, middle and inner ear implant, and dentomaxillofacial imaging. This technology is not without controversy, and further research is required to establish informed recommendations about its appropriate use in a clinical setting.

Acknowledgments

We thank Karen Carter for her help with image preparation; Sharon Brooks, for providing the images in figures 1 and 2; and Sylvia Miracle, for her review of the manuscript.

References

1. Robb RA. **The dynamic spatial reconstructor: an x-ray video-fluoroscopic CT scanner for dynamic volume imaging of moving organs.** *IEEE Trans Med Imaging* 1982;1:22–33
2. Fahrig R, Fox AJ, Lownie S, et al. **Use of a C-arm system to generate true three-dimensional computed rotational angiograms: preliminary in vitro and in vivo results.** *AJNR Am J Neuroradiol* 1997;18:1507–14
3. Saint-Félix D, Trousset Y, Picard C, et al. **In vivo evaluation of a new system for 3D computerized angiography.** *Phys Med Biol* 1994;39:583–95
4. Silver MD, Yahata M, Saito Y, et al. **Volume CT of anthropomorphic phantoms using a radiation therapy simulator.** In: Shaw R, ed. *Medical Imaging VI: Instrumentation: Proceedings of SPIE* 1992;1651:197–211
5. Cho PS, Johnson RH, Griffin TW. **Cone-beam CT for radiotherapy applications.** *Phys Med Biol* 1995:40:1863–83
6. Jaffray DA, Drake DG, Moreau M, et al. **A radiographic and tomographic imaging system integrated into a medical linear accelerator for localization of bone and soft-tissue targets.** *Int J Radiat Oncol Biol Phys* 1999;45:773–89
7. Daly MJ, Siewerdsen JH, Moseley DJ, et al. **Intraoperative cone-beam CT for guidance of head and neck surgery: assessment of dose and image quality using a C-arm prototype.** *Med Phys* 2006;33:3767–80
8. Rafferty MA, Siewerdsen JH, Chan Y, et al. **Intraoperative cone-beam CT for guidance of temporal bone surgery.** *Otolaryngol Head Neck Surg* 2006;134: 801–08
9. Siewerdsen JH, Moseley DJ, Burch S, et al. **Volume CT with a flat-panel detector on a mobile, isocentric C-arm: pre-clinical investigation in guidance of minimally invasive surgery.** *Med Phys* 2005;32:241–54
10. Khoury A, Siewerdsen JH, Whyne CM, et al. **Intraoperative cone-beam CT for image-guided tibial plateau fracture reduction.** *Comput Aided Surg* 2007;12: 195–207
11. Khoury A, Whyne CM, Daly M, et al. **Intraoperative cone-beam CT for correction of periaxial malrotation of the femoral shaft: a surface-matching approach.** *Med Phys* 2007;34:1380–87
12. Gupta R, Bartling SH, Basu SK, et al. **Experimental flat-panel high-spatial-resolution volume CT of the temporal bone.** *AJNR Am J Neuroradiol* 2004;25: 1417–24
13. Chen B, Ning R. **Cone-beam volume CT breast imaging: feasibility study.** *Med Phys* 2002;29:755–70
14. Peltonen LI, Aarnisalo AA, Kortesniemi MK, et al. **Limited cone-beam computed tomography imaging of the middle ear: a comparison with multislice helical computed tomography.** *Acta Radiol* 2007;48:207–12
15. Orth RC, Wallace MJ, Kuo MD, for the Technology Assessment Committee of the Society of Interventional Radiology. **C-arm cone-beam CT: general principles and technical considerations for use in interventional radiology.** *J Vasc Interv Radiol* 2008;19:814–20. Epub 2008 Apr 23
16. Dörfler A, Struffert T, Engelhorn T, et al. **Rotational flat-panel computed tomography in diagnostic and interventional neuroradiology.** *Rofo* 2008;180: 891–98
17. Moore CJ, Am A, Marchant T, et al. **Developments in and experience of kilovoltage X-ray cone beam image-guided radiotherapy.** *Br J Radiol* 2006;79(Spec No 1):S66–78
18. Scarfe WC, Farman AG, Sukovic P. **Clinical applications of cone-beam computed tomography in dental practice.** *J Can Dent Assoc* 2006;72:75–80
19. Glick SJ. **Breast CT.** *Annu Rev Biomed Eng* 2007;9:501–26
20. Mozzo P, Procacci C, Tacconi A, et al. **A new volumetric CT machine for dental imaging based on the cone-beam technique: preliminary results.** *Eur Radiol* 1998;8:1558–64
21. Arai Y, Tammisalo E, Iwai K, et al. **Development of a compact computed tomographic apparatus for dental use.** *Dentomaxillofac Radiol* 1999;28:245–48
22. Lascala CA, Panella J, Marques MM. **Analysis of the accuracy of linear measurements obtained by cone beam computed tomography (CBCT-NewTom).** *Dentomaxillofac Radiol* 2004;33:291–94
23. Mischkowski RA, Pulsfort R, Ritter L, et al. **Geometric accuracy of a newly developed cone-beam device for maxillofacial imaging.** *Oral Surg Oral Med Oral Pathol Oral Radiol Endod* 2007;104:551–59. Epub 2007 Jul 5
24. Lagravère MO, Carey J, Toogood RW, et al. **Three-dimensional accuracy of measurements made with software on cone-beam computed tomography images.** *Am J Orthod Dentofacial Orthop* 2008;134:112–16
25. Kumar V, Ludlow JB, Mol A, et al. **Comparison of conventional and cone beam CT synthesized cephalograms.** *Dentomaxillofac Radiol* 2007;36:263–69
26. Ludlow JB, Ivanovic M. **Comparative dosimetry of dental CBCT devices and 64-slice CT for oral and maxillofacial radiology.** *Oral Surg Oral Med Oral Pathol Oral Radiol Endod* 2008;106:106–14. Epub 2008 May 27
27. Schulze D, Heiland M, Thurmann H, et al. **Radiation exposure during midfacial imaging using 4- and 16-slice computed tomography, cone beam computed tomography systems and conventional radiography.** *Dentomaxillofac Radiol* 2004;33:83–86
28. Tyndall DA, Brooks SL. **Selection criteria for dental implant site imaging: a position paper of the American Academy of Oral and Maxillofacial Radiology.** *Oral Surg Oral Med Oral Pathol Oral Radiol Endod* 2000;89:630–37
29. Lofthag-Hansen S, Gröndahl K, Ekestubbe A. **Cone-beam CT for preoperative implant planning in the posterior mandible: visibility of anatomic landmarks.** *Clin Implant Dent Relat Res* 2008 Sep 9. [Epub ahead of print]
30. Guerrero ME, Jacobs R, Loubele M, et al. **State-of-the-art on cone beam CT imaging for preoperative planning of implant placement.** *Clinical Oral Investig* 2006;10:1–7
31. Ito K, Gomi Y, Sato S, et al. **Clinical application of a new compact CT system to assess 3-D images for the preoperative treatment planning of implants in the posterior mandible: a case report.** *Clin Oral Implants Res* 2001;12:539–42
32. Sato S, Arai Y, Shinoda K, et al. **Clinical application of a new cone-beam computerized tomography system to assess multiple two-dimensional images for the preoperative treatment planning of maxillary implants: case reports.** *Quintessence Int* 2004;35:525–28
33. Terakado M, Hashimoto K, Arai Y, et al. **Diagnostic imaging with newly developed ortho cubic super-high resolution computed tomography (Ortho-CT).** *Oral Surg Oral Med Oral Pathol Oral Radiol Endod* 2000;89:509–18
34. Ziegler CM, Woertche R, Brief J, et al. **Clinical indications for digital volume**

tomography in oral and maxillofacial surgery. *Dentomaxillofac Radiol* 2002;31:126–30

35. Drage NA, Sivarajasingam V. **The use of cone beam computed tomography in the management of isolated orbital floor fractures.** *Br J Oral Maxillofac Surg* 2009;47:65–66. Epub 2008 Jun 30
36. Zizelmann C, Gellrich NC, Metzger MC, et al. **Computer-assisted reconstruction of orbital floor based on cone beam tomography.** *Br J Oral Maxillofac Surg* 2007;45:79–80. Epub 2005 Aug 10
37. Heiland M, Schulze D, Blake F, et al. **Intraoperative imaging of zygomaticomaxillary complex fractures using a 3D C-arm system.** *Int J Oral Maxillofac Surg* 2005;34:369–75
38. Pohlenz P, Blessmann M, Blake F, et al. **Clinical indications and perspectives for intraoperative cone-beam computed tomography in oral and maxillofacial surgery.** *Oral Surg Oral Med Oral Pathol Oral Radiol Endod* 2007;103:412–17. Epub 2006 Sep 26
39. Heiland M, Schulze D, Rother U, et al. **Postoperative imaging of zygomaticomaxillary complex fractures using digital volume tomography.** *J Oral Maxillofac Surg* 2004;62:1387–91
40. Pohlenz P, Blessmann M, Blake F, et al. **Major mandibular surgical procedures as an indication for intraoperative imaging.** *J Oral Maxillofac Surg* 2008;66:324–29
41. Holberg C, Steinhauser S, Geis P, et al. **Cone-beam computed tomography in orthodontics: benefits and limitations** [in English, German]. *J Orofac Orthop* 2005;66:434–44
42. Gracco A, Lombardo L, Cozzani M, et al. **Quantitative cone-beam computed tomography evaluation of palatal bone thickness for orthodontic miniscrew placement.** *Am J Orthod Dentofacial Orthop* 2008;134:361–69
43. King KS, Lam EW, Faulkner MG, et al. **Vertical bone volume in the paramedian palate of adolescents: a computed tomography study.** *Am J Orthod Dentofacial Orthop* 2007;132:783–88
44. Garrett BJ, Caruso JM, Rungcharassaeng K, et al. **Skeletal effects to the maxilla after rapid maxillary expansion assessed with cone-beam computed tomography.** *Am J Orthod Dentofacial Orthop* 2008;134:8–9
45. Yang F, Jacobs R, Willems G. **Dental age estimation through volume matching of teeth imaged by cone-beam CT.** *Forensic Sci Int* 2006;159(suppl 1):S78–83. Epub 2006 Mar 23
46. Aboudara CA, Hatcher D, Nielsen IL, et al. **A three-dimensional evaluation of the upper airway in adolescents.** *Orthod Craniofac Res* 2003;6(suppl 1):173–75
47. Nakajima A, Sameshima GT, Arai Y, et al. **Two- and three-dimensional orthodontic imaging using limited cone beam-computed tomography.** *Angle Orthod* 2005;75:895–903
48. Silva MA, Wolf U, Heinicke F, et al. **Cone-beam computed tomography for routine orthodontic treatment planning: a radiation dose evaluation.** *Am J Orthod Dentofacial Orthop* 2008;133:640.e1–5
49. Brooks SL, Brand JW, Gibbs SJ, et al. **Imaging of the temporomandibular joint: a position paper of the American Academy of Oral and Maxillofacial Radiology.** *Oral Surg Oral Med Oral Pathol Oral Radiol Endod* 1997;83:609–18
50. Hintze H, Wiese M, Wenzel A. **Cone beam CT and conventional tomography for the detection of morphological temporomandibular joint changes.** *Dentomaxillofac Radiol* 2007;36:192–97
51. Honda K, Arai Y, Kashima M, et al. **Evaluation of the usefulness of the limited cone-beam CT (3DX) in the assessment of the thickness of the roof of the glenoid fossa of the temporomandibular joint.** *Dentomaxillofac Radiol* 2004;33:391–95
52. Honda K, Larheim TA, Maruhashi K, et al. **Osseous abnormalities of the mandibular condyle: diagnostic reliability of cone beam computed tomography compared with helical computed tomography based on an autopsy material.** *Dentomaxillofac Radiol* 2006;35:152–57
53. Honey OB, Scarfe WC, Hilgers MJ, et al. **Accuracy of cone-beam computed tomography imaging of the temporomandibular joint: comparisons with panoramic radiology and linear tomography.** *Am J Orthod Dentofacial Orthop* 2007;132:429–38
54. Hussain AM, Packota G, Major PW, et al. **Role of different imaging modalities in assessment of temporomandibular joint erosions and osteophytes: a systematic review.** *Dentomaxillofac Radiol* 2008;37:63–71
55. Patel S, Dawood A, Ford TP, et al. **The potential applications of cone beam computed tomography in the management of endodontic problems.** *Int Endod J* 2007;40:818–30. Epub 2007 Aug 14
56. Lofthag-Hansen S, Huumonen S, Gröndahl K, et al. **Limited cone-beam CT and intraoral radiography for the diagnosis of periapical pathology.** *Oral Surg Oral Med Oral Pathol Oral Radiol Endod* 2007;103:114–19. Epub 2006 Apr 24
57. Nakata K, Naitoh M, Izumi M, et al. **Effectiveness of dental computed tomography in diagnostic imaging of periradicular lesion of each root of a multirooted tooth: a case report.** *J Endod* 2006;32:583–87
58. Low KM, Dula K, Bürgin W, von Arx T. **Comparison of periapical radiography and limited cone-beam tomography in posterior maxillary teeth referred for apical surgery.** *J Endod* 2008;34:557–62
59. Rigolone M, Pasqualini D, Bianchi L, et al. **Vestibular surgical access to the palatine root of the superior first molar: "low-dose cone-beam" CT analysis of the pathway and its anatomic variations**. *J Endod* 2003;29:773–35
60. Ito K, Yoshinuma N, Goke E, et al. **Clinical application of a new compact computed tomography system for evaluating the outcome of regenerative therapy: a case report.** *J Periodontol* 2001;72:696–702
61. Mengel R, Candir M, Shiratori K, et al. **Digital volume tomography in the diagnosis of periodontal defects: an in vitro study on native pig and human mandibles.** *J Periodontol* 2005;76:665–73
62. Misch KA, Yi ES, Sarment DP. **Accuracy of cone beam computed tomography for periodontal defect measurements.** *J Periodontol* 2006;77:1261–66
63. Vandenberghe B, Jacobs R, Yang J. **Diagnostic validity (or acuity) of 2D CCD versus 3D CBCT-images for assessing periodontal breakdown.** *Oral Surg Oral Med Oral Pathol Oral Radiol Endod* 2007;104:395–401. Epub 2007 Jul 5
64. Mol A, Balasundaram A. **In vitro cone beam computed tomography imaging of periodontal bone.** *Dentomaxillofac Radiol* 2008;37:319–24
65. Vandenberghe B, Jacobs R, Yang J. **Detection of periodontal bone loss using digital intraoral and cone beam computed tomography images: an in vitro assessment of bony and/or infrabony defects.** *Dentomaxillofac Radiol* 2008;37:252–60
66. Ozmeric N, Kostioutchenko I, Hagler G, et al. **Cone-beam computed tomography in assessment of periodontal ligament space: in vitro study on artificial tooth model.** *Clin Oral Investig* 2008;12:233–39. Epub 2008 Feb 5
67. Rafferty MA, Siewerdsen JH, Chan Y, et al. **Investigation of C-arm cone-beam CT-guided surgery of the frontal recess.** *Laryngoscope* 2005;115:2138–43
68. Chennupati SK, Woodworth BA, Palmer JN, et al. **Intraoperative IGS/CT updates for complex endoscopic frontal sinus surgery.** *ORL J Otorhinolaryngol Relat Spec* 2008;70:268–70. Epub 2008 May 19
69. Alspaugh J, Christodoulou E, Goodsitt M, et al. **Dose and image quality of flat-panel detector volume computed tomography for sinus imaging.** In: *Proceedings of the 49th Annual Meeting of the American Association of Physics in Medicine,* Minneapolis, Minn. July 22–26, 2007
70. Jackman AH, Palmer JN, Chiu AG, et al. **Use of intraoperative CT scanning in endoscopic sinus surgery: a preliminary report.** *Am J Rhinol* 2008;22:170–74
71. Batra PS, Kanowitz SJ, Citardi MJ. **Clinical utility of intraoperative volume computed tomography scanner for endoscopic sinonasal and skull base procedures.** *Am J Rhinol* 2008;22:511–15
72. Harvey RJ, Goddard JC, Wise SK, et al. **Effects of endoscopic sinus surgery and delivery device on cadaver sinus irrigation.** *Otolaryngol Head Neck Surg* 2008;139:137–42
73. Hudgins PA, Browning DG, Gallups J, et al. **Endoscopic paranasal sinus surgery: radiographic evaluation of severe complications.** *AJNR Am J Neuroradiol* 1992;13:1161–67
74. Zinreich SJ. **Functional anatomy and computed tomography imaging of the paranasal sinuses.** *Am J Med Sci* 1998;316:2–12
75. Cerini R, Faccioli N, Barillari M, et al. **Bionic ear imaging.** *Radiol Med* 2008;113:265–77. Epub 2008 Apr 2
76. Yamane H, Takayama M, Sunami K, et al. **Three-dimensional images of the reuniting duct using cone beam CT.** *Acta Otolaryngol* 2009;129:493–96
77. Husstedt HW, Aschendorff A, Richter B, et al. **Nondestructive three-dimensional analysis of electrode to modiolus proximity.** *Otol Neurotol* 2002;23:49–52
78. Richter B, Aschendorff A, Lohnstein P, et al. **The Nucleus Contour electrode array: a radiological and histological study.** *Laryngoscope* 2001;111:508–14
79. Aschendorff A, Kubalek R, Hochmuth A, et al. **Imaging procedures in cochlear implant patients: evaluation of different radiological techniques.** *Acta Otolaryngol Suppl* 2004;552:46–49
80. Offergeld C, Kromeier J, Aschendorff A, et al. **Rotational tomography of the normal and reconstructed middle ear in temporal bones: an experimental study.** *Eur Arch Otorhinolaryngol* 2007;264:345–51. Epub 2006 Oct 18
81. Aschendorff A, Kubalek R, Turowski B, et al. **Quality control after cochlear implant surgery by means of rotational tomography.** *Otol Neurotol* 2005;26:34–47
82. Dalchow CV, Weber AL, Bien S, et al. **Value of digital volume tomography in patients with conductive hearing loss.** *Eur Arch Otorhinolaryngol* 2006;263:92–99. Epub 2005 Sep 15
83. Chong V. **The skull base in oncologic imaging.** *Cancer Imaging* 2004;4:5–6
84. Bachar G, Siewerdsen JH, Daly MJ, et al. **Image quality and localization accuracy in C-arm tomosynthesis-guided head and neck surgery.** *Med Phys* 2007;34:4664–77
85. Bartling SH, Leinung M, Graute J, et al. **Increase of accuracy in intraoperative navigation through high-resolution flat-panel volume computed tomography: experimental comparison with multislice computed tomography-based navigation.** *Otol Neurotol* 2007;28:129–34
86. Woodworth BA, Chiu AG, Cohen NA, et al. **Real-time computed tomography image update for endoscopic skull base surgery.** *J Laryngol Otol* 2008;122:361–65. Epub 2007 Aug 16
87. Mukherji SK, Gujar S, Jordan JE, et al. **ACR Practice Guideline for the Performance of Computed Tomography (CT) of the Extracranial Head and Neck in Adults and Children.** *ACR Practice Guideline* 2006 (Res 12,17,35). Available at: http://www.acr.org/SecondaryMainMenuCategories/quality_safety/guidelines/dx/head-neck/ct_head_neck.aspx. Accessed January 15, 2009
88. Carter L, Farman AG, Geist J, et al. **American Academy of Oral and Maxillofacial Radiology executive opinion statement on performing and interpreting diagnostic cone beam computed tomography.** *Oral Surg Oral Med Oral Pathol Oral Radiol Endod* 2008;106:561–62